Synthesis and Characterization of Nanostructured Spinel Ferrites

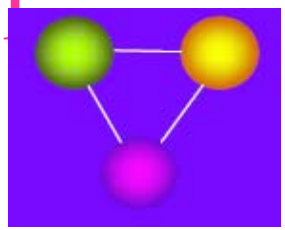

Muhammad Javed Iqbal
Department of Chemistry
Quaid-i-Azam University
Islamabad

NANOSCIENCE

- Average human hair 25000 nm wide
- Molecules with 30 atoms have 1 nm diameter
- Human cells range from 5000 – 200,000 nm
- Proteins ---------- 3-20 nm
- Viruses --------- 10-200 nm
- Drugs used to fight virus < 5 nm

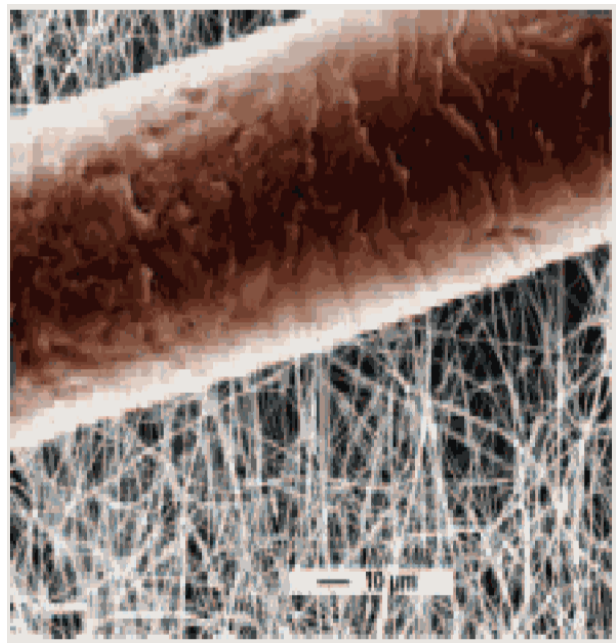

Nanotechnology

- Creation of functional (novel) materials, devices and systems through control of matter on nanometer length scale ~ 1-100 nm range. 100 nm is not an arbitrary dividing line
- The deviation of properties of nanosized materials from bulk materials properties are due to surface effects (S/V ratio, particle size, etc.)
- Motivations in nanoscience is to understand how materials behave when sample sizes are close to atomic dimensions.
- When characteristic length scale of microstructure is 1-100 nm it becomes comparable with the critical length scales of biological/physical phenomena – so called "size and shape effects"

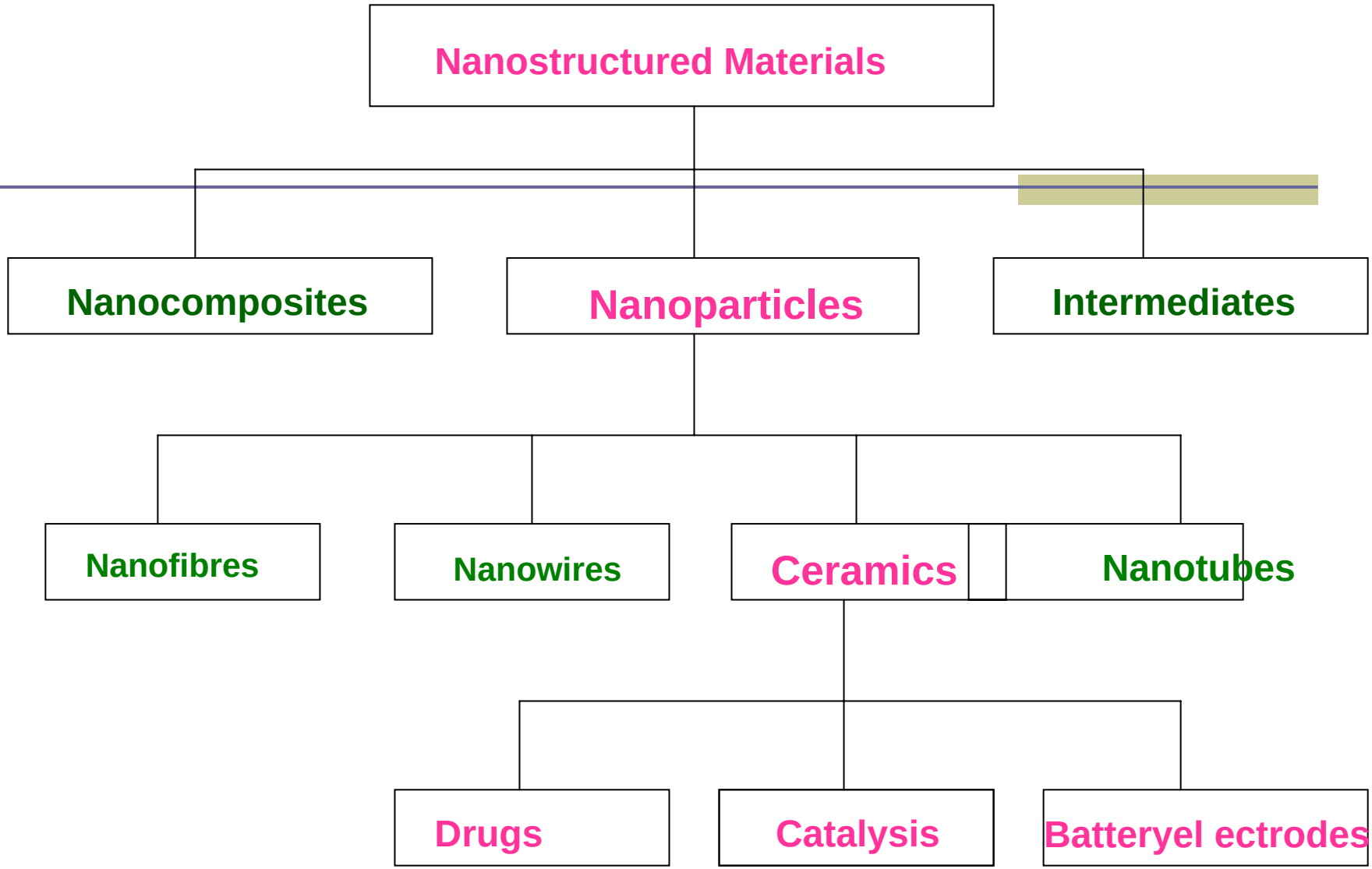
Nanostructured Materials
Nanocomposites
Nanoparticles
Intermediates
Nanofibres
Nanowires
Ceramics
Nanotubes
Drugs
Catalysis
Batteryel ectrodes

Themes of Nanotechnology

- the bottom-up approach

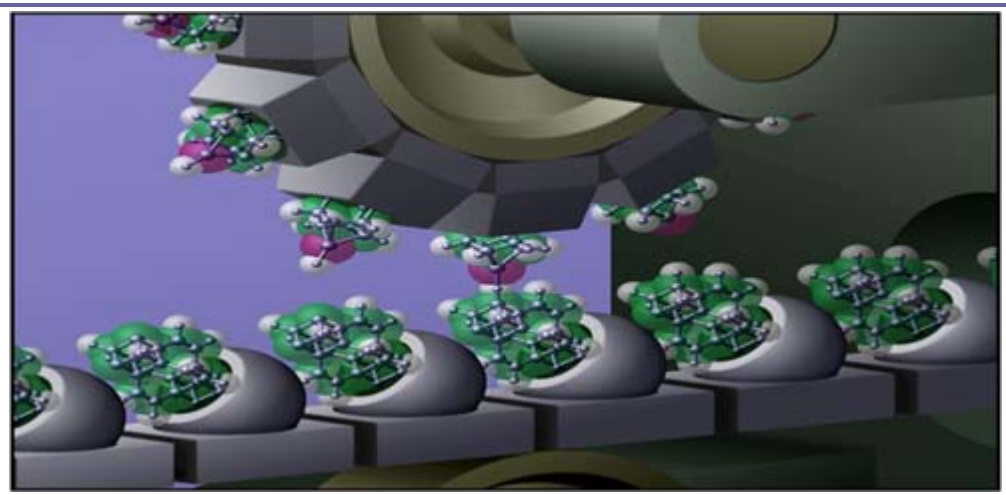

- the top-down approach

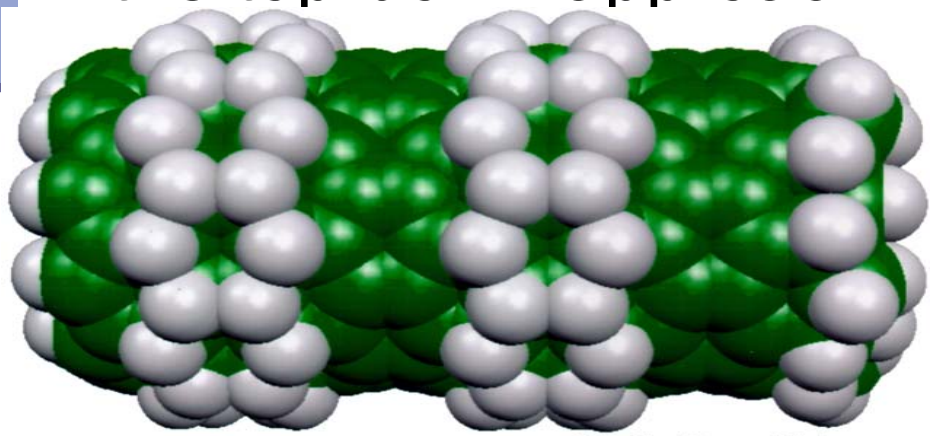

Spinel

- Great imposter of gemstone history
- Famous rubies in crown jewels (SPINELS)

BLACK PRINCE'S RUBY

Spinel Gallery

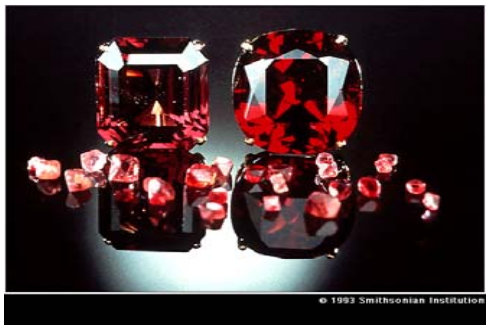

Spinel Compounds

- General formula $A[B_2]O_4$
  - A divalent metal ions Fe^{2+}, Mg^{2+}, Ni^{2+}
  - B Trivalent metal ions Fe^{3+},Cr^{3+},$Al^{3+,}$ Mn^{3+}
- Cubic close packing of O^{2-} ions
- Two types of sites
  - Octahedral sites (B-sites)
  - Tetrahedral sites (A-sites)

Structure of Spinel

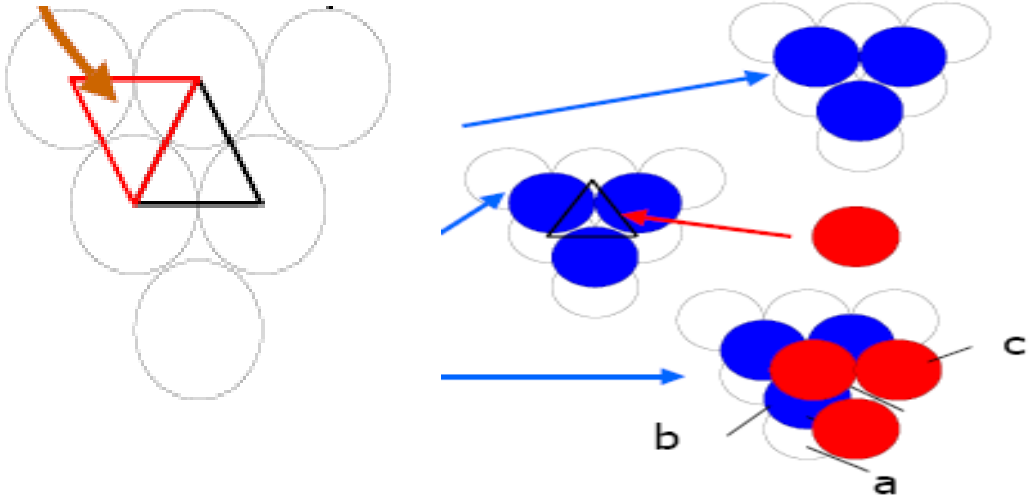

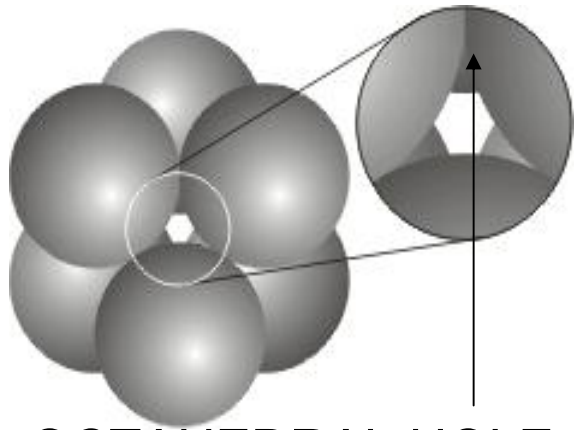

OCTAHEDRAL HOLE

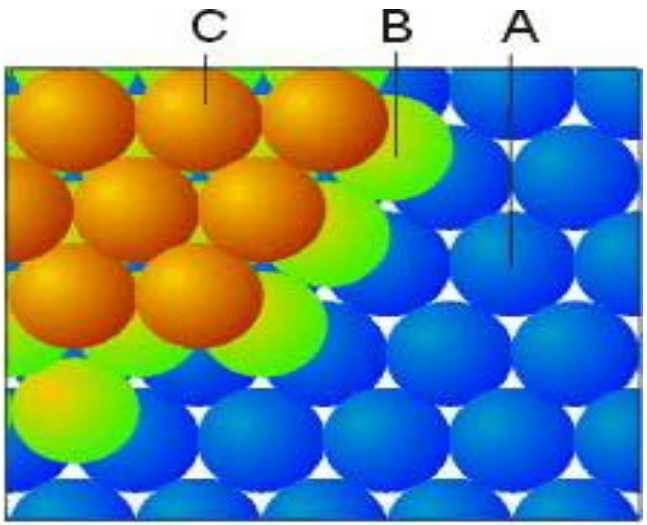

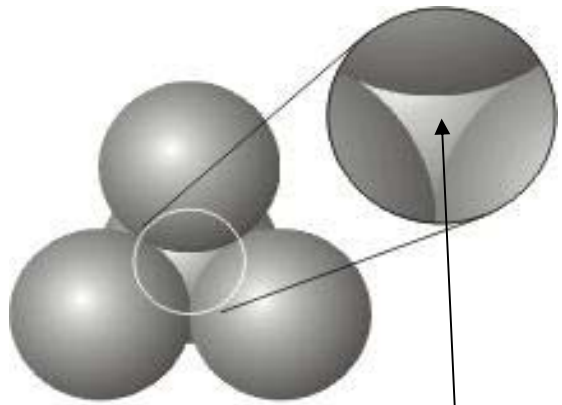

TETRAHEDRAL HOLE

Classification of Spinels

- NORMAL SPINEL $(A)^{tet}\ [B_2]^{oct}\ O_4$

  e.g. $(Mg)[Al_2]O_4$, $(Zn)[Fe_2]O_4$

- INVERSE SPINEL $(B)^{tet}\ [A, B]^{oct}\ O_4$

  e.g. $(Fe)[Fe]O_4$, $(Fe)[NiFe]O_4$

- RANDOM SPINEL $(B_{0.67}\ A_{0.33})^{tet}\ [A_{0.67}B_{1.33}]^{oct}O_4$

Types of Magnetic Interactions

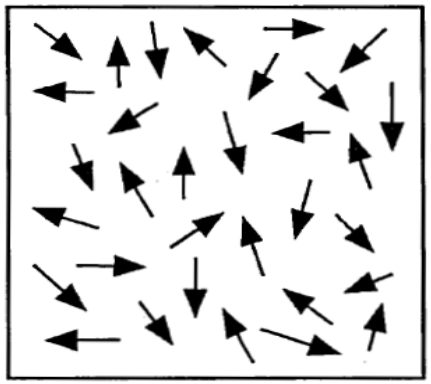

Paramagnetism

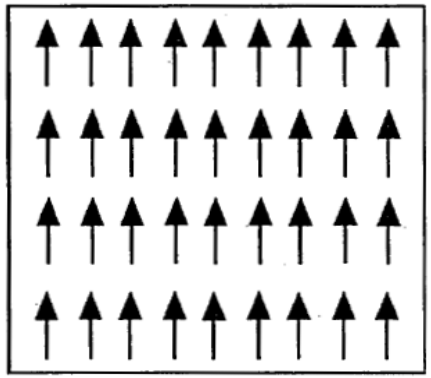

Ferromagnetism

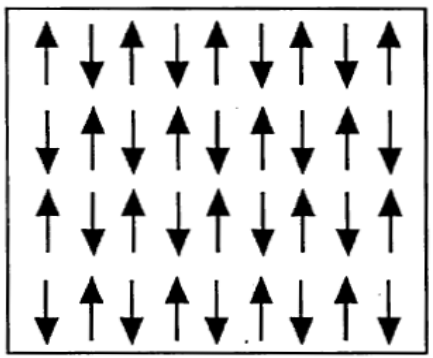

Anti-ferromagnetism

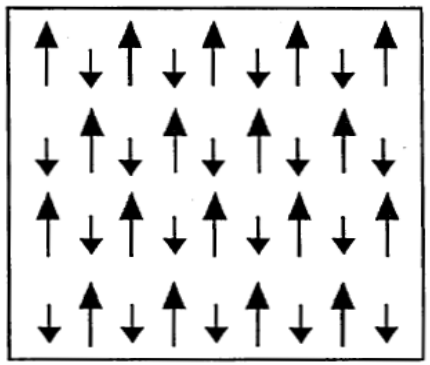

Ferrimagnetisms

Why Cobalt Ferrite ($CoFe_2O_4$)?

- Perfect chemical stability (metal & alloys unstable under atmospheric conditions)
- Good thermal stability
- High electrical resistivity (high frequency devices, memory cores, recording media)
- High saturation magnetization (high density recording media)
- Low coercivity (for recording and reading of data)
- Super-exchange interaction
- Super-paramagnetism (Biomedical applications)

Applications

- Medical applications
  - Magnetic Resonance Imaging (MRI)
  - Targeted drug delivery
  - Hyperthermia for cancer treatment
- High density storage devices
- Magnetic fluids
- Transformer cores
- Microwave devices
- Humidity and Gas Sensors

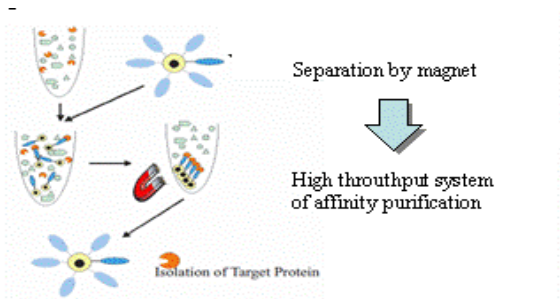

Aims & Objectives

- To obtain stable, single phase ferrites at different temperatures.
- To synthesize cobalt ferrites with a size ~ 70 nm; more suitable for use in recording devices.
- To enhance the electrical resistivity from $>10^7$ Ωcm to consequently decrease eddy current losses & dielectric constant (ε) for use as transformer cores
- To crease the Curie Temperature (Tc)
- To increase the coercivity $H_c \sim$ 600-1000 Oe for applications in recording media

Experimental

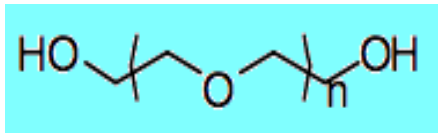

- Micro-emulsion method using Poly ethylene glycol (PEG) as surfactant
- Surfactant makes nano-reactors for the formation of the product
- NH_3 (35%) solution is used to maintain pH=9.5

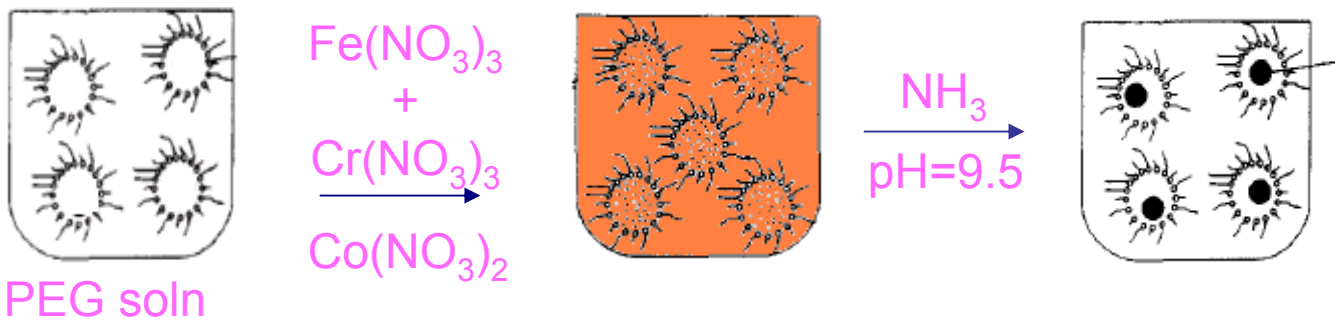

- E.Goldman, Modern Ferrite Technology, 2nd ed., Springer, Pittsburgh USA 2006

Mechanism of Ferrite Formation

$$(2\text{-}x)Fe(NO_3)_3 + xMe(NO_3)_2 + Co(NO_3)_2 + 8NaOH(aq)$$

PEG ↓ pH=9.5

$$(2\text{-}x)Fe(OH)_3.Co(OH)_2.xMe(OH)_2.nH_2O + 8NaNO_3$$

Drying at 120 & annealing at 800°C ↓ 5°C/min

$CoFe_{2-x}Me_xO_4$ (Me = Zr^{4+}, Mg^{2+})

(Spinel Ferrite)

Characterization Techniques

- Thermogravimetric Analysis TG/DTA (Perkin Elmer)
- X-ray Diffraction XRD Analysis (PANalytical 3040/60 X'Pert PRO)
- Energy Dispersive X-ray Fluorescence ED-XRF (Horiba MESA-500)
- Scanning Electron microscopy SEM (Hitachi VP S3400N)
- DC-Electrical Resistivity Measurements by two probe method (Lab made setup)
- Dielectric measurements (Wayne Kerr LCR4275)
- AC-Susceptibility at 273 Hz (Lab made setup)
- Magnetic measurements using AC-induction method

Parameters Calculated by XRD

$$a = \left[d^2 (h^2 + k^2 + l^2) \right]^{1/2}$$

$$D = \frac{K \lambda}{\beta \, Cos \, \theta}$$

K = shape factor (0.9), β = FWHM
λ = 1.54 Å

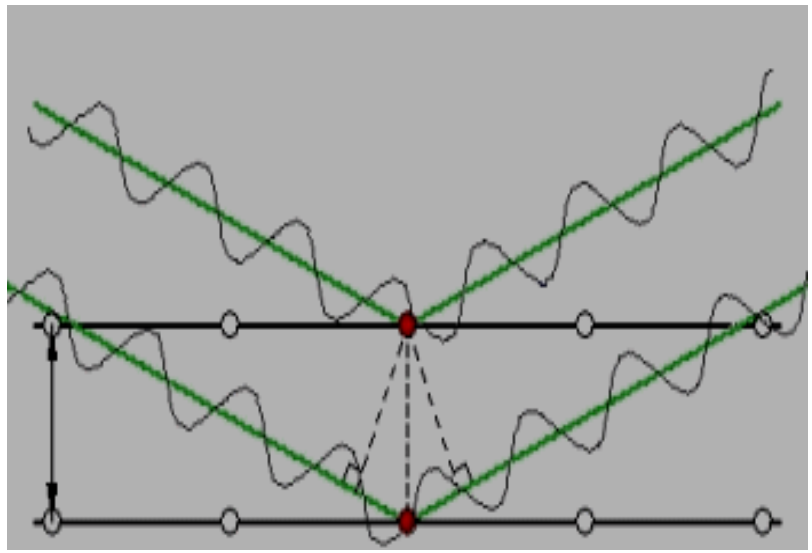

$$d_{x-ray} = \frac{ZM}{N_A V_{cell}}$$

Z= no. formula units (8), M=Molar mass

DC Electrical Resistivity Apparatus

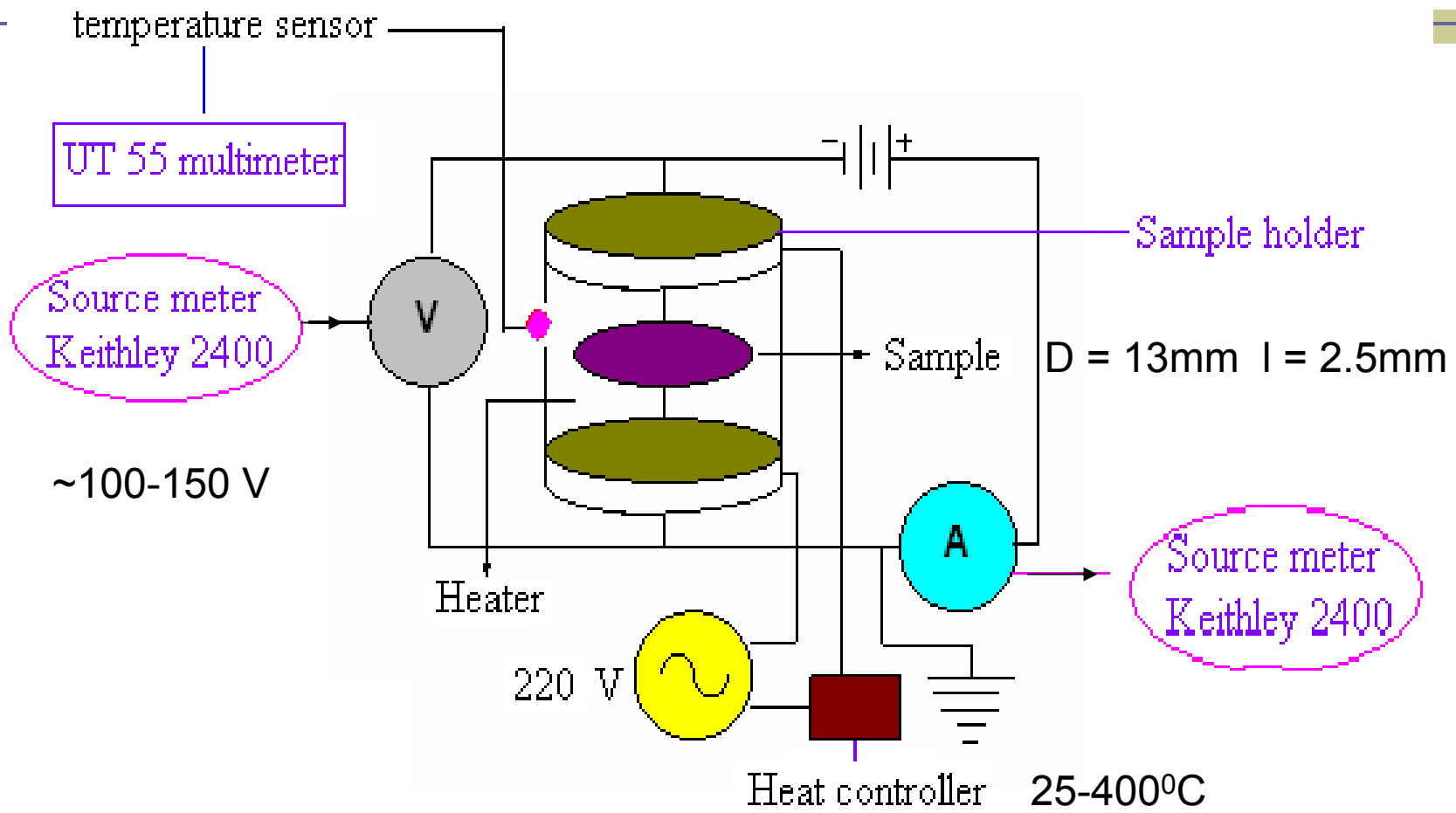

Resistivity Parameters

Resistivity is calculated by the formula:

$$V = IR \quad ; \qquad \rho = R\frac{A}{L}$$

where R is the resistance, $A = \pi r^2$ is area and L is the width of the pellet, r = 6.5mm

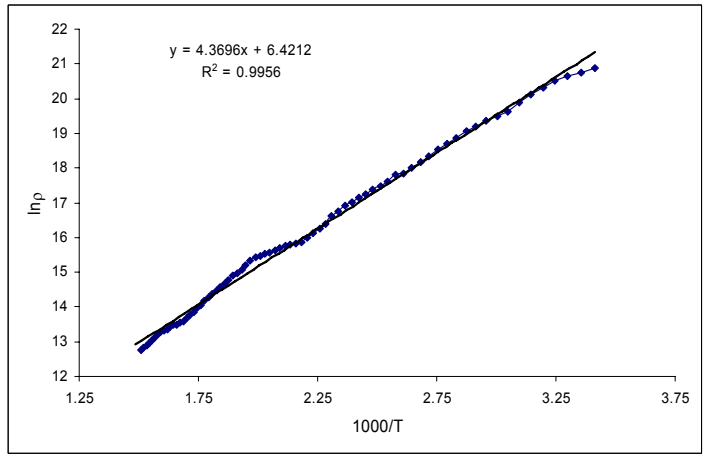

Resistivity shows exponential dependence on temperature and is given by Arrhenius-type Equation

$$\rho = \rho_0 \exp\left(\frac{E_a}{k_B T}\right)$$

Activation energy of hopping (Ea) is calculated by plotting resistivity vs 1000/T

Dielectric Parameters

- Dielectric constant can be calculated by

$$\acute{\epsilon} = C\ d/\epsilon_o A$$

C = Capacitance, d = thickness, A = Cross-sectional area and ϵ_o is the permittivity constant of free space (lit.)

- Dielectric loss is given as

$$\text{Tan}\delta = 1/2\pi f R_p C$$

R_p = Equivalent parallel resistivity

C_p = Equivalent parallel capacitance

f = Applied frequency

AC Magnetic Susceptibility Apparatus

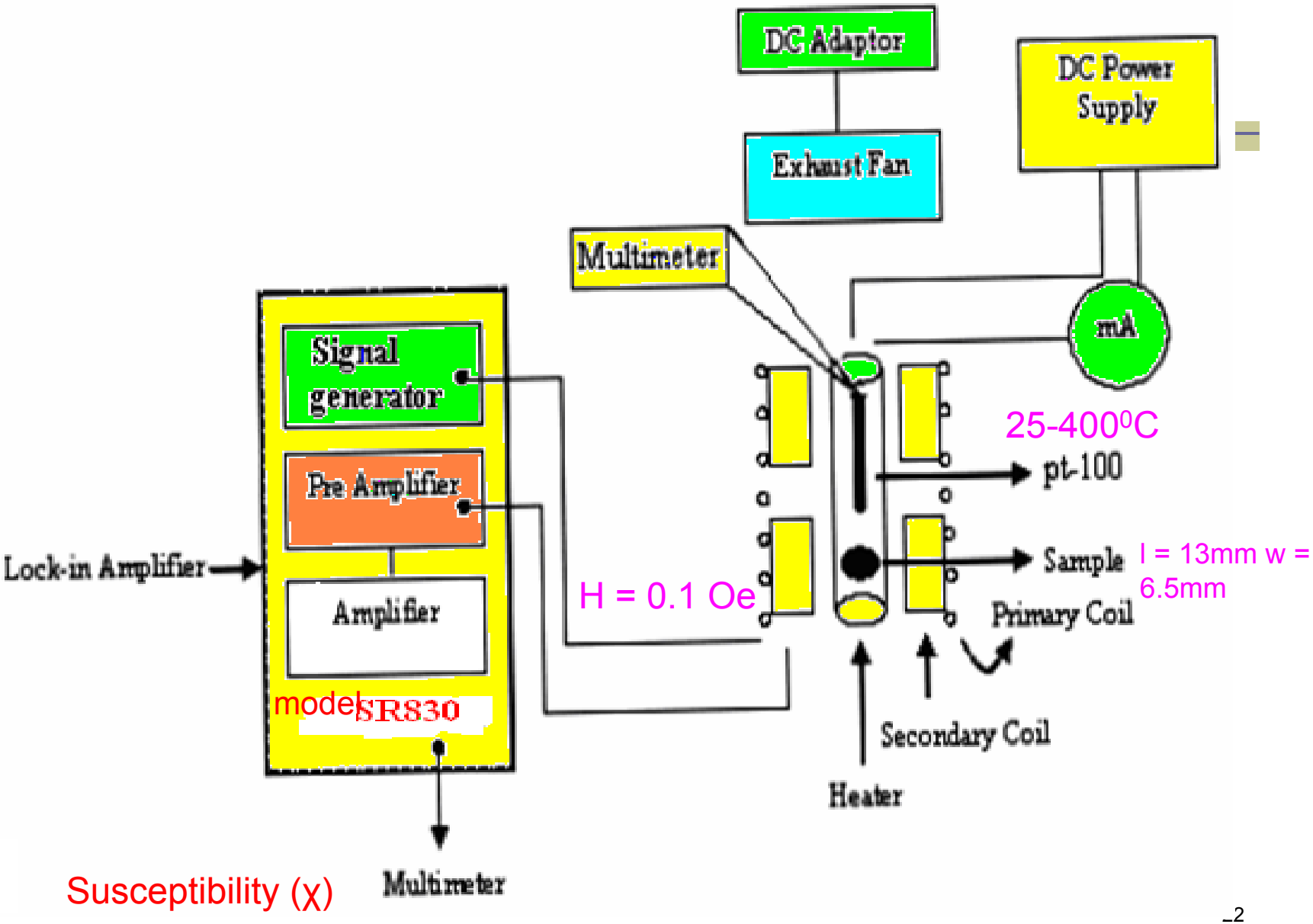

Susceptibility (χ)

Susceptibility vs Temperature

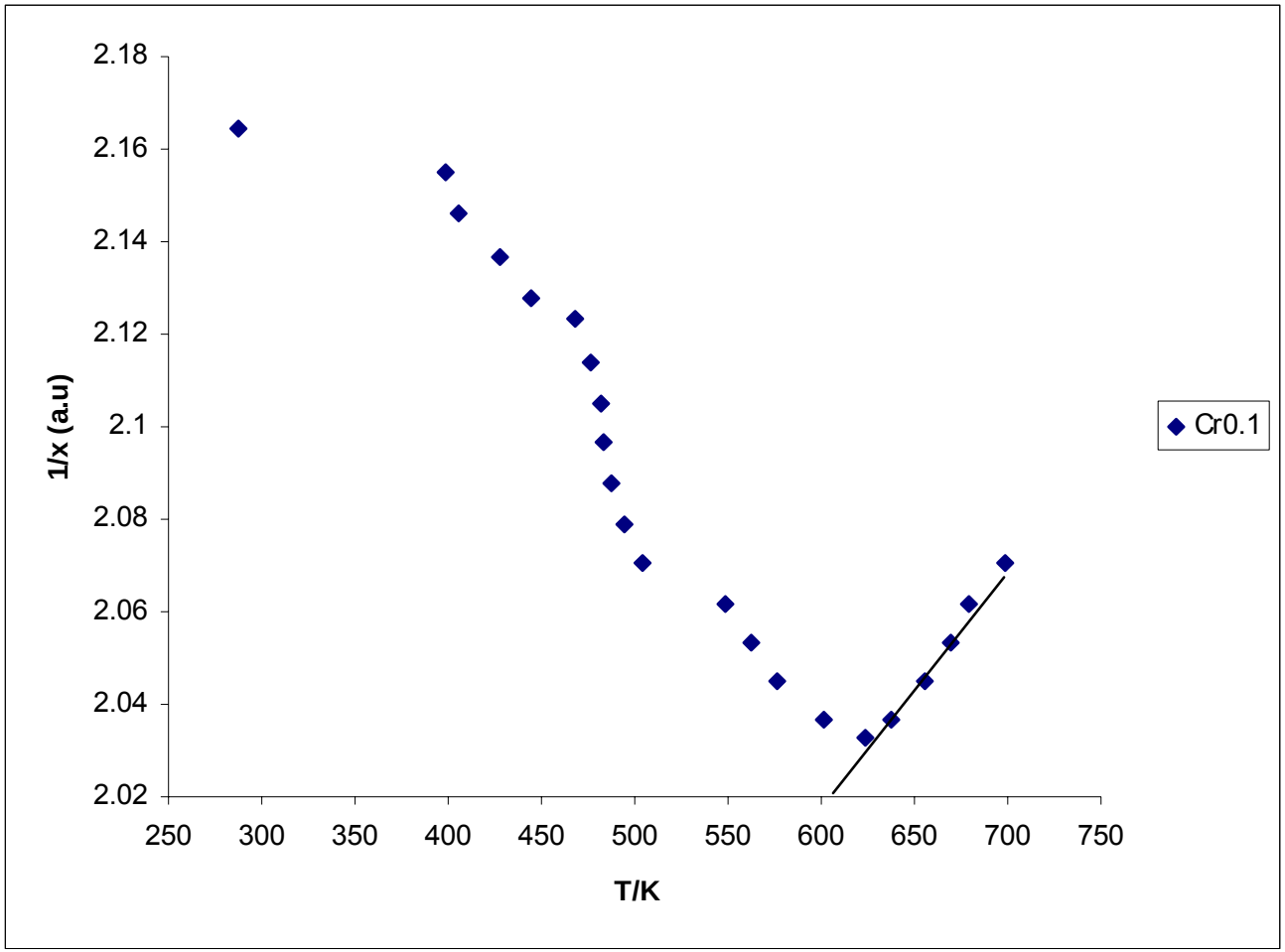

Hysteresis loops for Cr doped cobalt ferrite

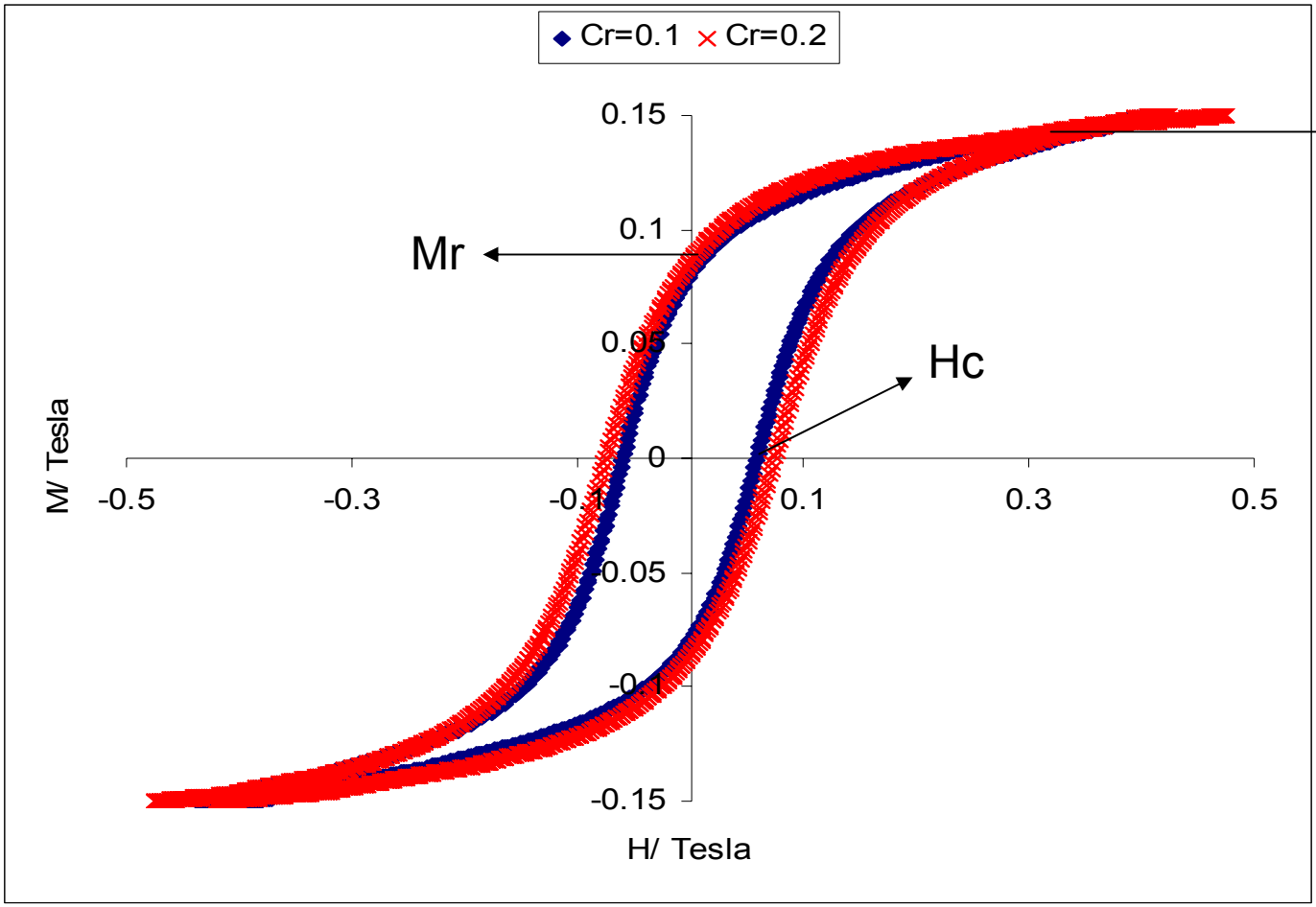

Magnetic Parameters

- Magnetic moment (n_B) can be calculated by the formula:

$$n_B = \frac{Mol.wt. \times M_s}{5.585 d_b}$$

where M_s is saturation magnetization, d_b is the bulk density.

- Yafet-Kittle angles ($\alpha_{Y\text{-}K}$) are determined from the value of n_B and dopant content 'x':

$$n_B = (6 + x)\cos\alpha_{Y-K} - 5(1 - x)$$

XRD patterns of $CoCr_xFe_{2-x}O_4$(x = 0.0 -1.0)

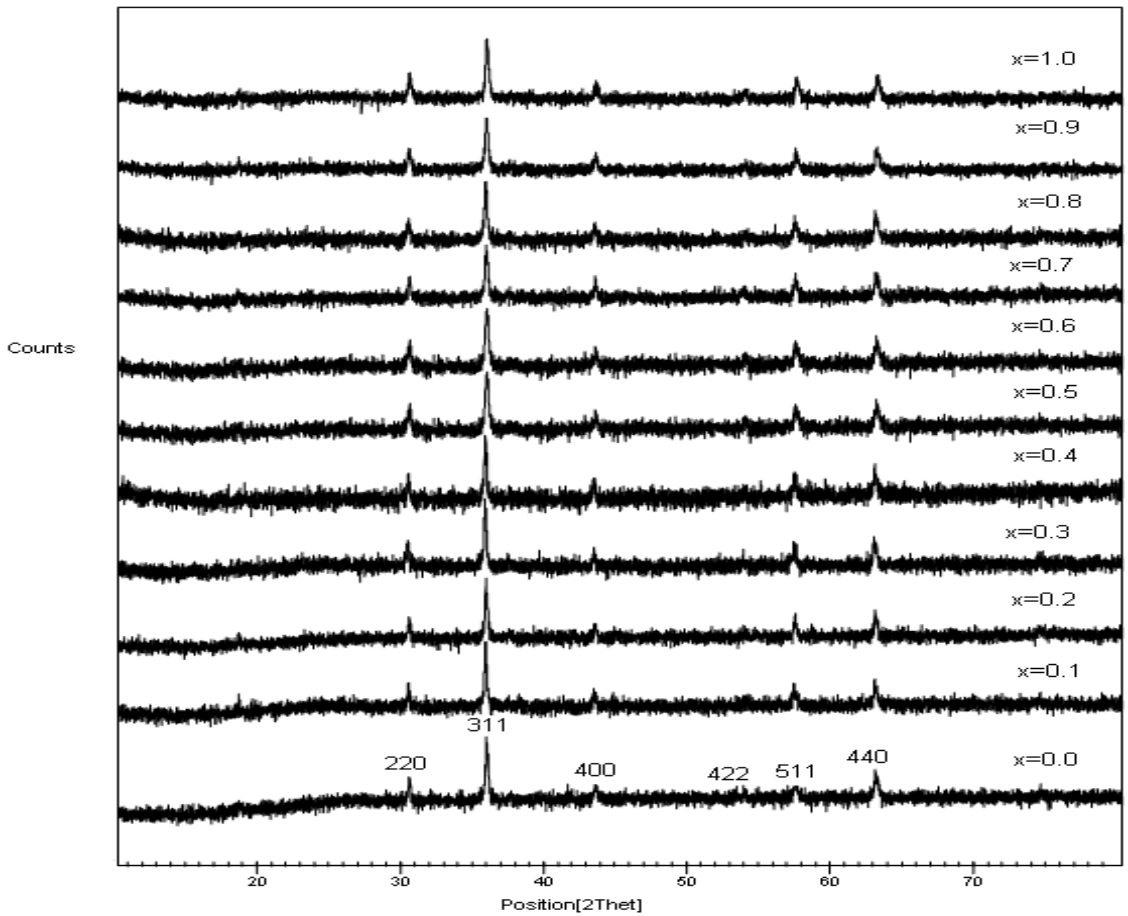

SEM of $CoCr_{0.1}Fe_{1.9}O_4$

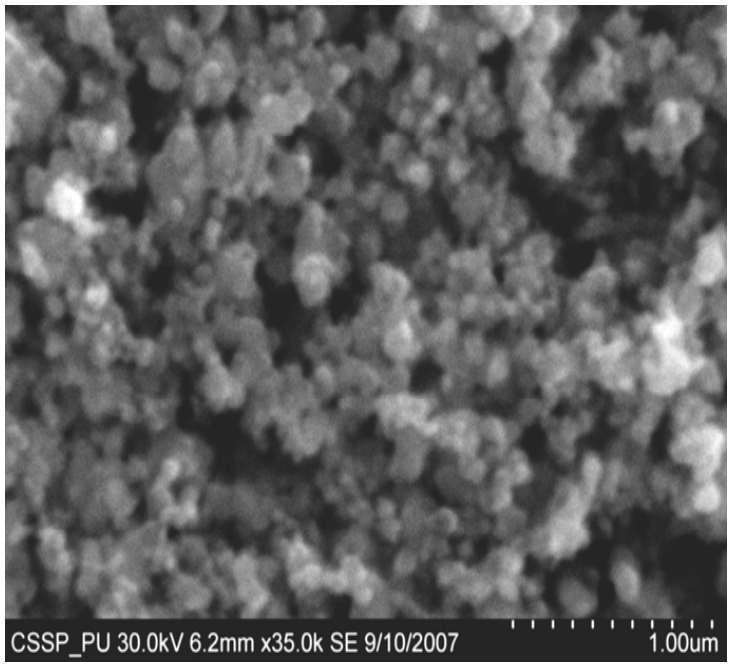

Different parameters calculated for Co (Cr_x Fe_{2-x}) O_4 samples

Cr content 'x'	D (nm)	a (±0.001 Å)	d_x (±0.01 gcm^{-3})	p	mol (±0.01)			T_C (±1 K)	ε
					Cr	Fe	Co		
		(8.38)	(5.12)					(793)	
0.0	20	8.385	5.12	0.33	0.00	2.10	1.08	600	88.62
0.1	73	8.383	5.33	0.48	0.09	1.80	1.11	615	63.50
0.2	62	8.381	5.55	0.44	0.19	1.72	1.09	**635**	60.95
0.3	65	8.375	5.77	0.44	0.28	1.63	1.09	595	59.41
0.4	49	8.373	5.98	0.48	0.36	1.54	1.09	575	53.49
0.5	66	8.369	6.20	0.51	0.46	1.44	1.09	610	45.91
0.6	53	8.368	6.42	0.54	0.59	1.31	1.10	540	43.85
0.7	40	8.366	6.63	0.57	0.66	1.24	1.10	420	39.85
0.8	70	8.364	6.85	0.60	0.73	1.17	1.09	410	39.49
0.9	49	8.356	7.08	0.62	0.84	1.18	0.98	355	24.93
1.0	49	8.355	7.29	0.65	0.95	1.16	0.90	312	**21.32**

Plot of resistivity at 393K and activation energy (Ea) versus chromium content in cobalt ferrites

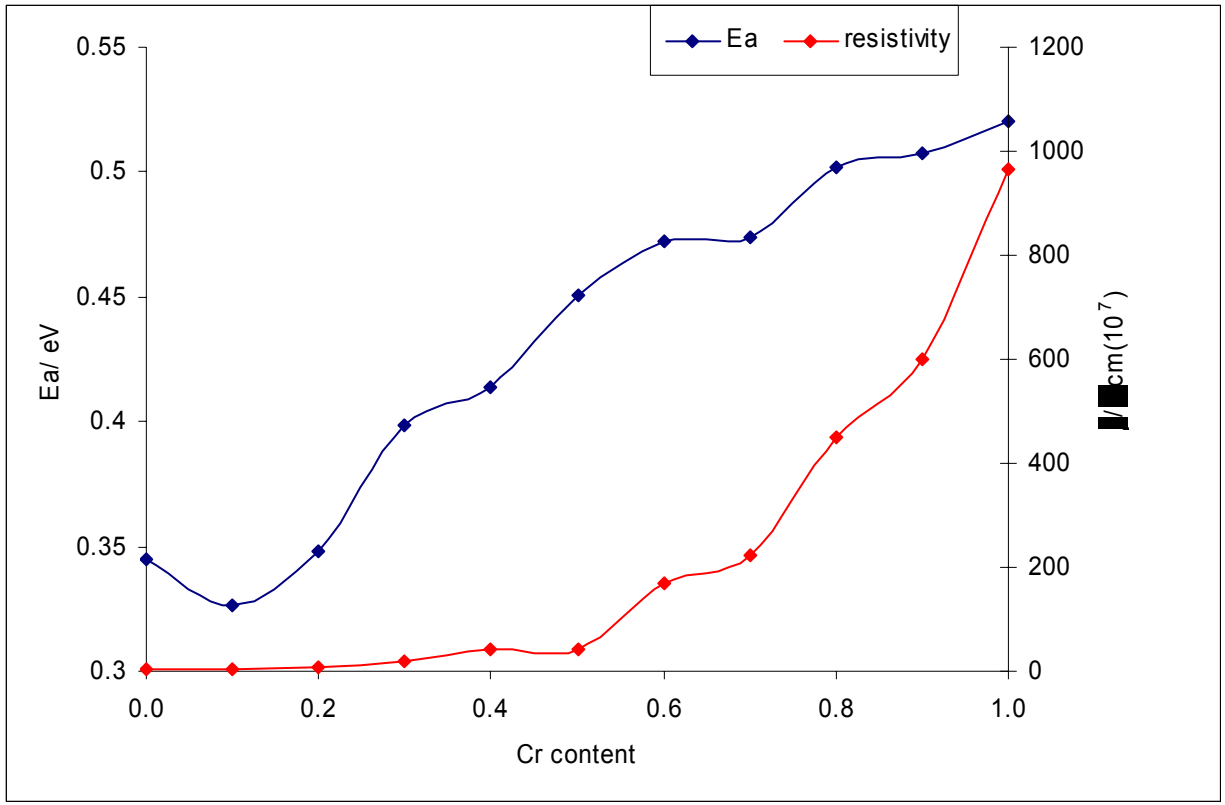

Ea=0.345-0.520 eV

$\rho=5.59\times10^{7}$-$9.66\times10^{9}\ \Omega$cm;

p-type conductivity

Electrical Properties of Spinel Ferrites

$$\rho = \rho_0 \exp\left(\frac{E_a}{k_B T}\right)$$

- Hopping at octahedral (B-sites)

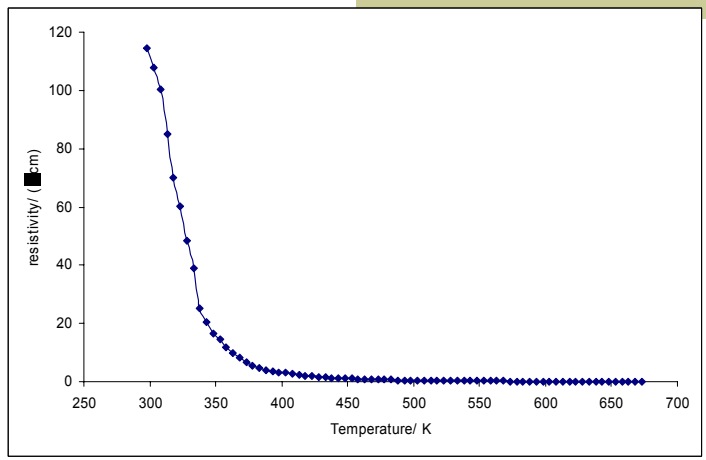

$$Fe^{2+} + Fe^{3+} \leftrightarrow Fe^{3+} + Fe^{2+}$$

$$(Fe^{3+})[Fe^{2+}Fe^{3+}]O_4^{2-} = (Fe^{3+})[Fe^{3+}Fe^{2+}]O_4^{2-}$$

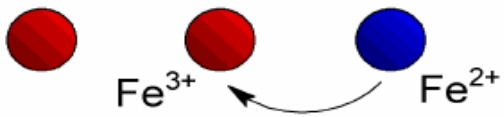

$$Me^{2+} + Fe^{3+} \leftrightarrow Me^{3+} + Fe^{2+}$$

$$(Fe^{3+})[Me^{2+}Fe^{3+}]O_4^{2-} \neq (Fe^{3+})[Me^{3+}Fe^{2+}]O_4^{2-}$$

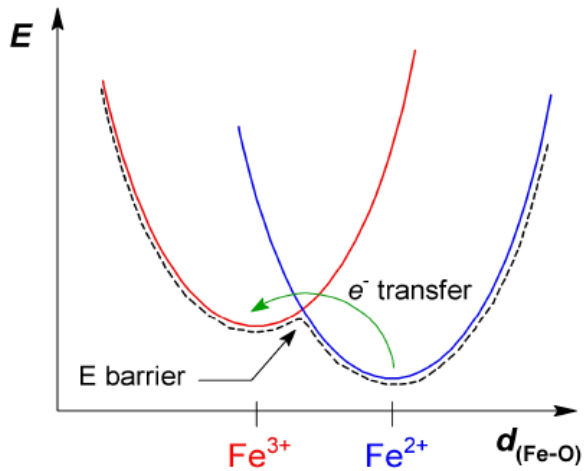

Magnetic parameters of chromium substituted cobalt ferrite determined from hysteresis loops

Cr	$M_s(kAm^{-1})$	$M_r(kAm^{-1})$	Hc (Oe)
	(81.61)	(50.96)	(879.2)
0.1	119.43	66.08	859.10
0.2	111.46	63.69	814.24
0.4	87.58	50.96	646.19*
0.6	63.69	34.24	388.74
0.8	51.75	19.90	254.44
1.0	19.90	4.54	57.27

Magnetic Properties of Spinel Ferrites

An Anti-parallel arrangement of the ions at tetrahedral (A-site) and octahedral sites (B-sites)

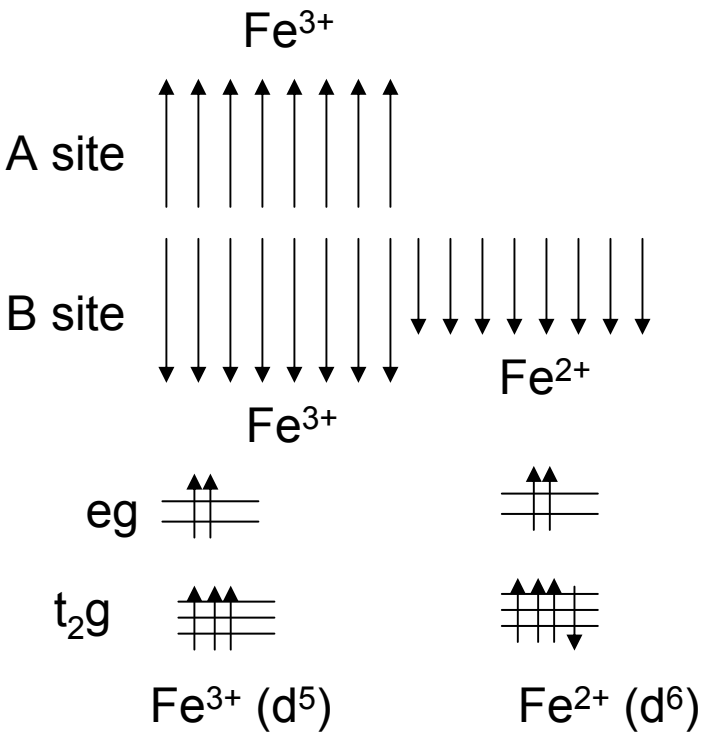

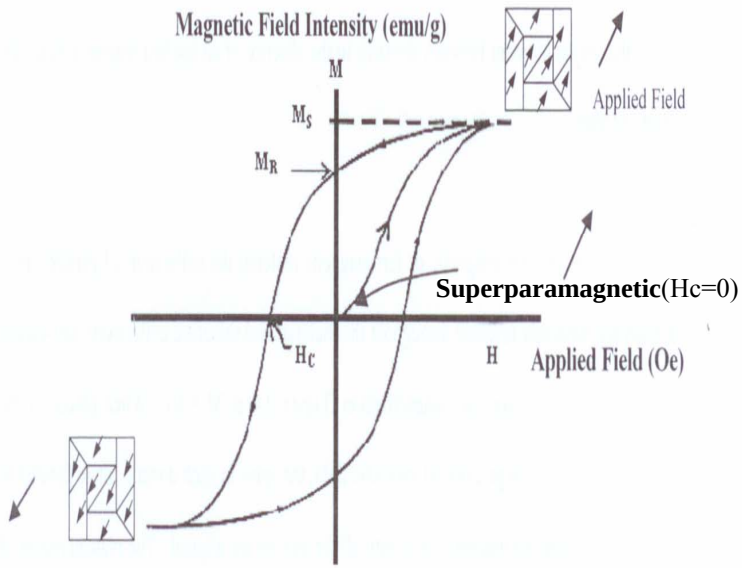

Plot of saturation magnetization (Ms) and coercivity (Hc) versus chromium content in cobalt ferrites

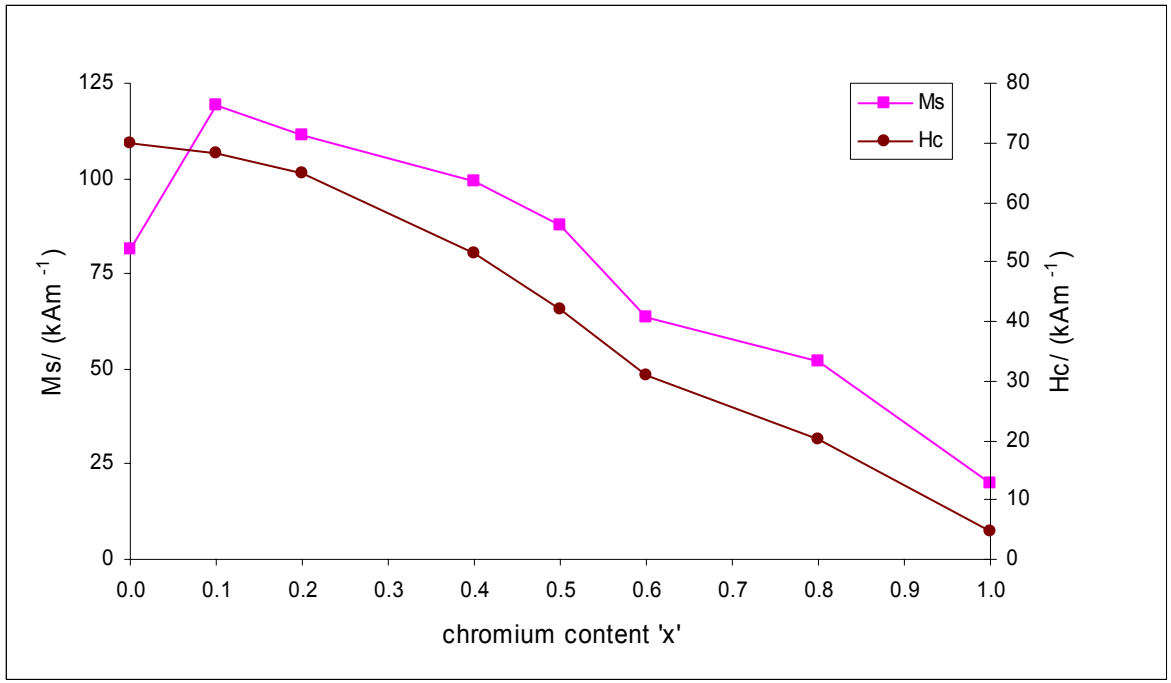

Ms= 81-19.90 kAm^{-1}(80.8 emu/g)

Hc= 70-4.56 kAm^{-1}

Models for Magnetic Interactions

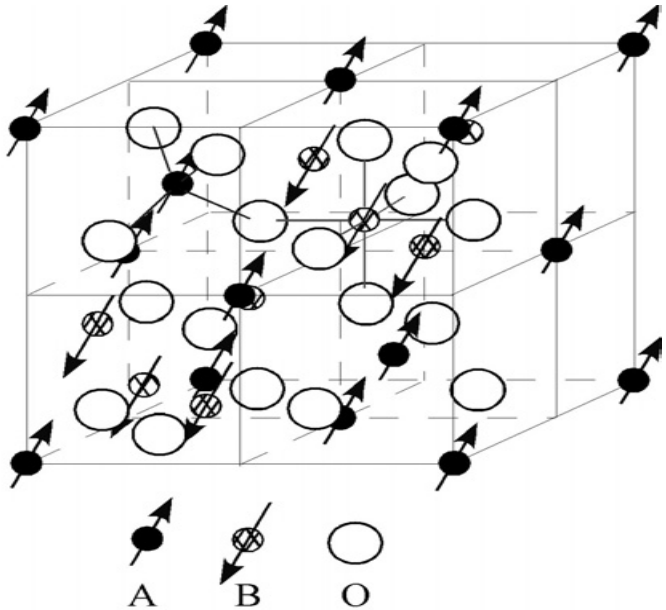

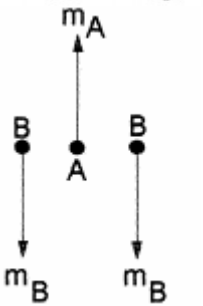

Neel's Model

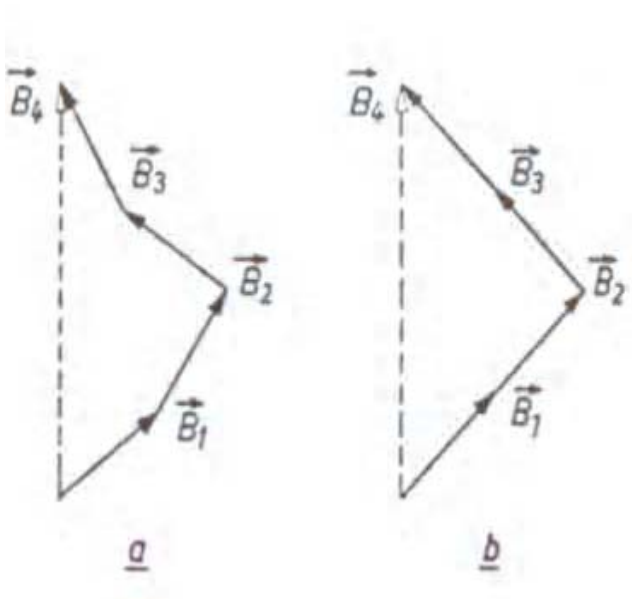

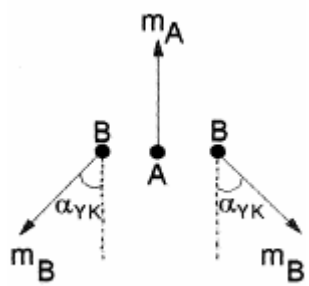

Yafet-Kittle Model

Calculated Y-K angles of chromium substituted cobalt ferrites

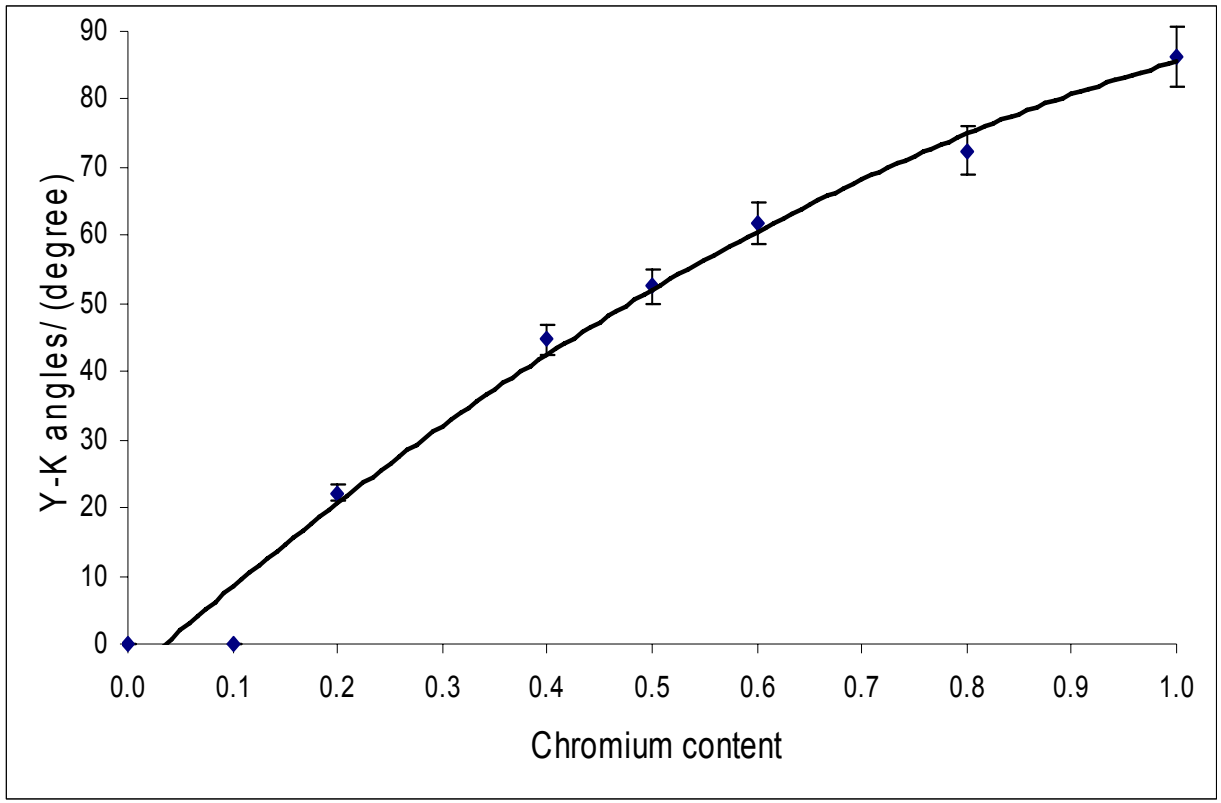

Conclusions for Cr doped series

- All the samples synthesized are single phase
- Lattice parameter 'a' decreased from 8.385 to 8.355Å with increase in chromium content, x, from 0 -0.1
- Resistivity increases with increase (5.59×10^{7}-9.66×10^{9} Ωcm) in chromium content and is more suitable for use in high density recording devices
- The activation energy of hopping increases from 0.345-0.520 eV with addition of chromium from 0 - 0.1
- The Curie temperature has increased for x≤0.2 (600K to 635K) and then decreases with increase in chromium concentration
- Maximum Ms value (119 kAm^{-1}) is observed for Cr = 0.1. Neel's model of sublattices is applicable for pure and Cr = 0.1 doped cobalt ferrite.
- For Cr = 0.2 -1.0 Yafet-Kittle model of triangular sublattices is applicable and the canting angle varies from 24^{o}-86^{o}.

M. J. Iqbal; M.R. Siddiquah, *J. Alloy. Comp. 453 (2008) 513-518*

Zr-Mg Doped Cobalt Ferrite

XRD patterns of $CoZr_xMg_xFe_{2-2x}O_4$

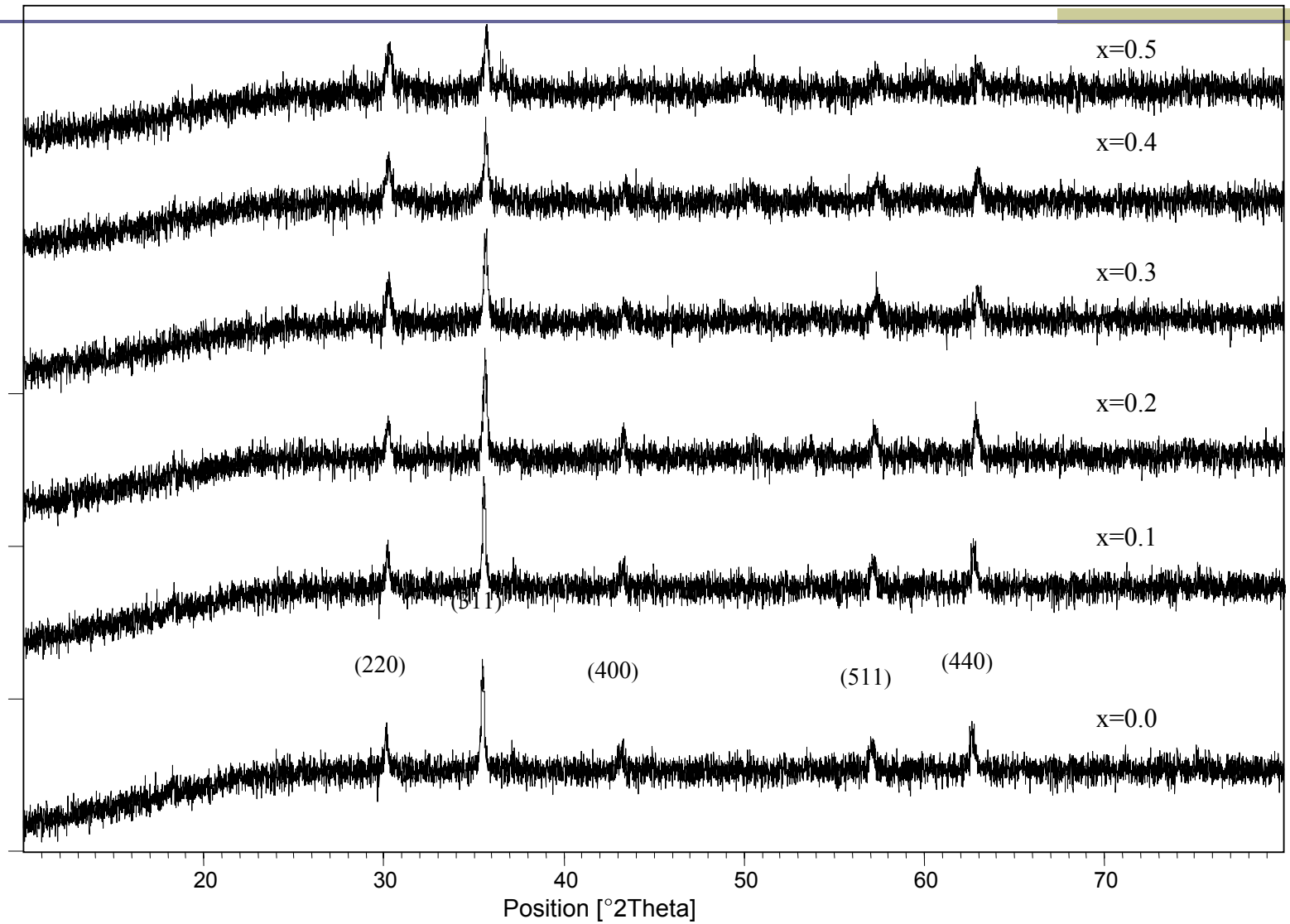

Calculated values of lattice parameter (a), crystallite size (D), X-ray density (dx), porosity (p), dielectric constant (έ) and remanence (Mr) of $CoMg_xZr_xFe_{2-2x}O_4$ (x = 0.0-0.5)

x	D (nm)	a (±0.001 gcm^{-3})	d_x (±0.01 gcm^{-3})	p	mol			T_C (±1 K)	ε	Mr (kAm^{-1})
					Zr	Fe	Mg			
0.0	20	8.385	5.12	0.33	0.00	2.10	0.00	600	88.62	50.96
0.1	52	8.387	5.12	0.46	0.09	1.80	0.04	625	94.62	31.85
0.2	53	8.364	5.17	0.41	0.20	1.72	0.11	620	76.52	22.29
0.3	47	8.350	5.21	0.46	0.26	1.63	0.21	555	84.27	15.92
0.4	47	8.343	5.23	0.46	0.37	1.54	0.32	525	116.46	14.33
0.5	35	8.339	5.24	0.39	0.46	1.44	0.39	520	109.99	13.93

SEM images of Zr-Mg substituted cobalt ferrites

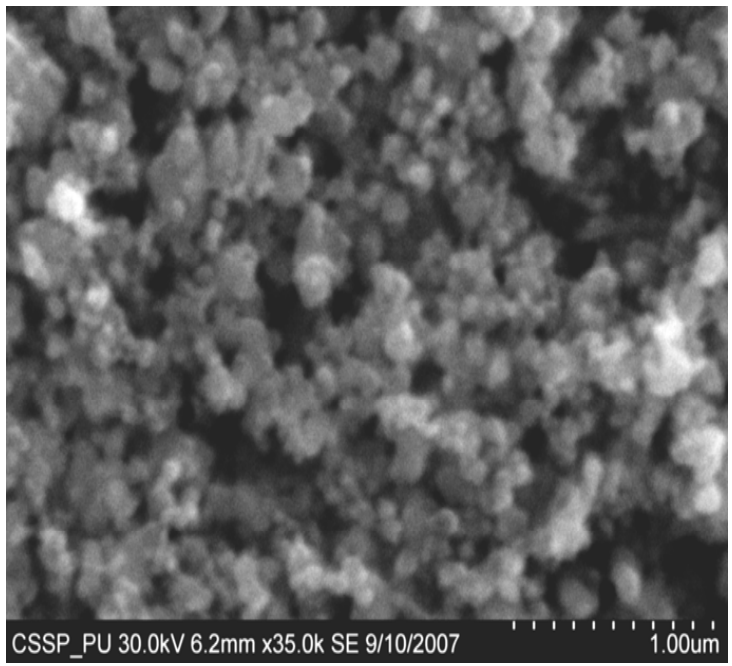

Zr/Mg=0.1

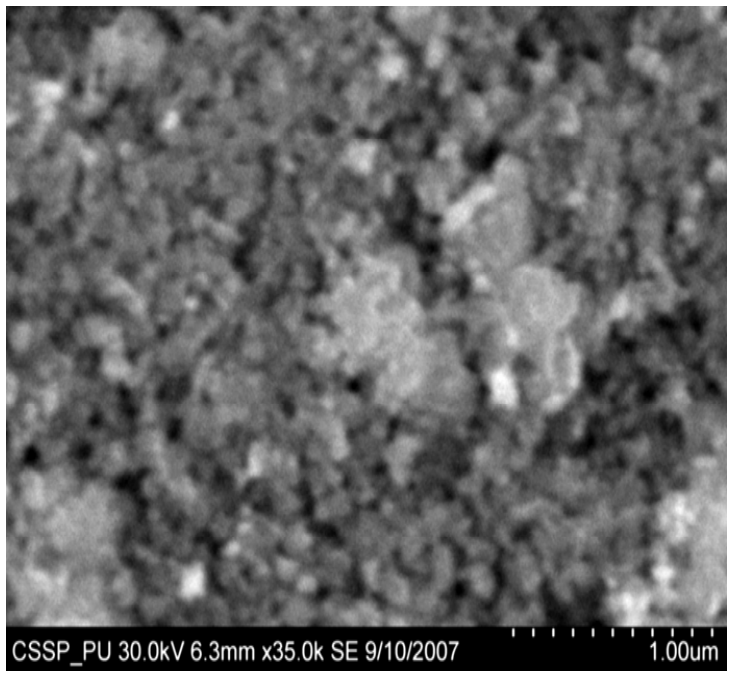

Zr/Mg=0.5

Plot of resistivity at 293K and activation energy (Ea) versus Zr/Mg content in cobalt ferrites

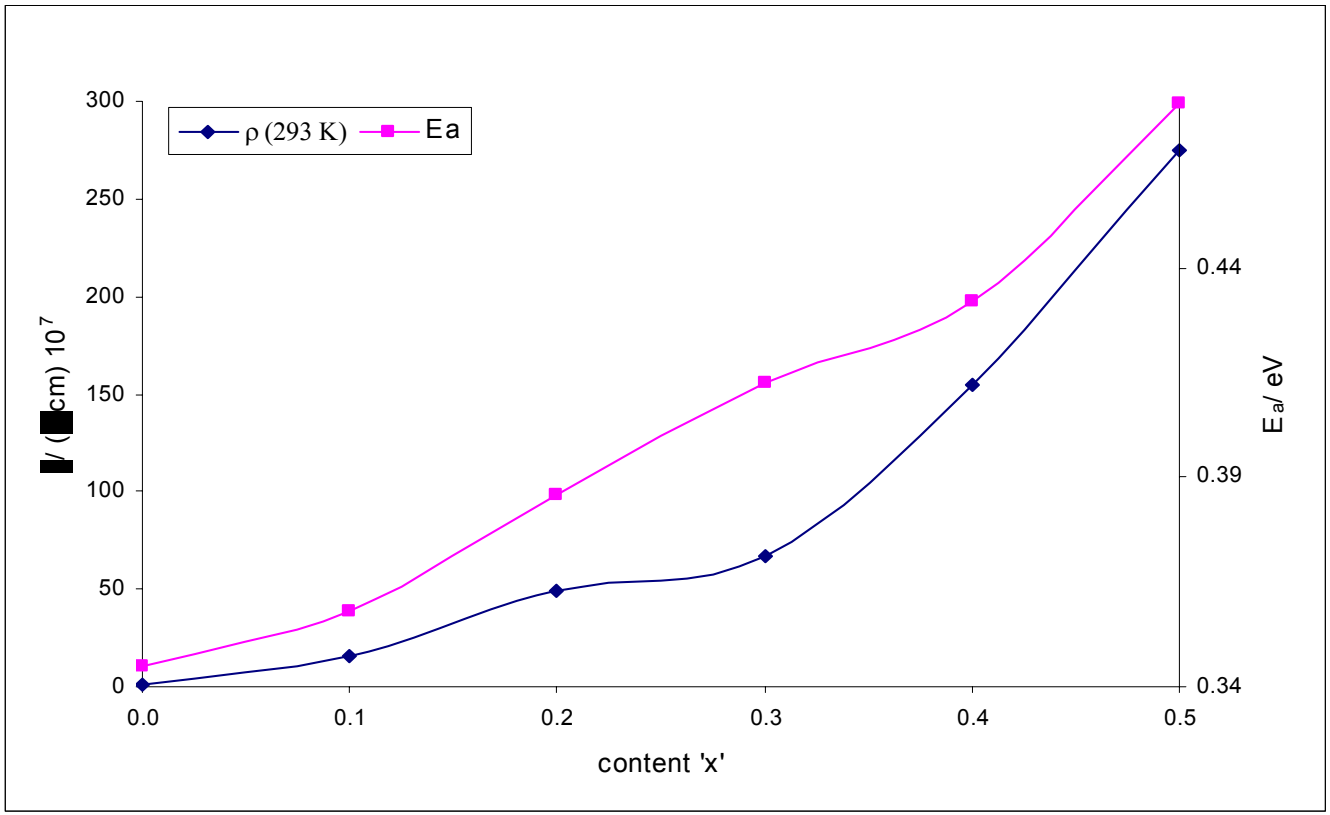

Ea = 0.34-0.48 eV

p= 5.59×10^{7}-2.75×10^{9} Ωcm

Plot of saturation magnetization (Ms) and coercivity versus Zr/Mg content in cobalt ferrites

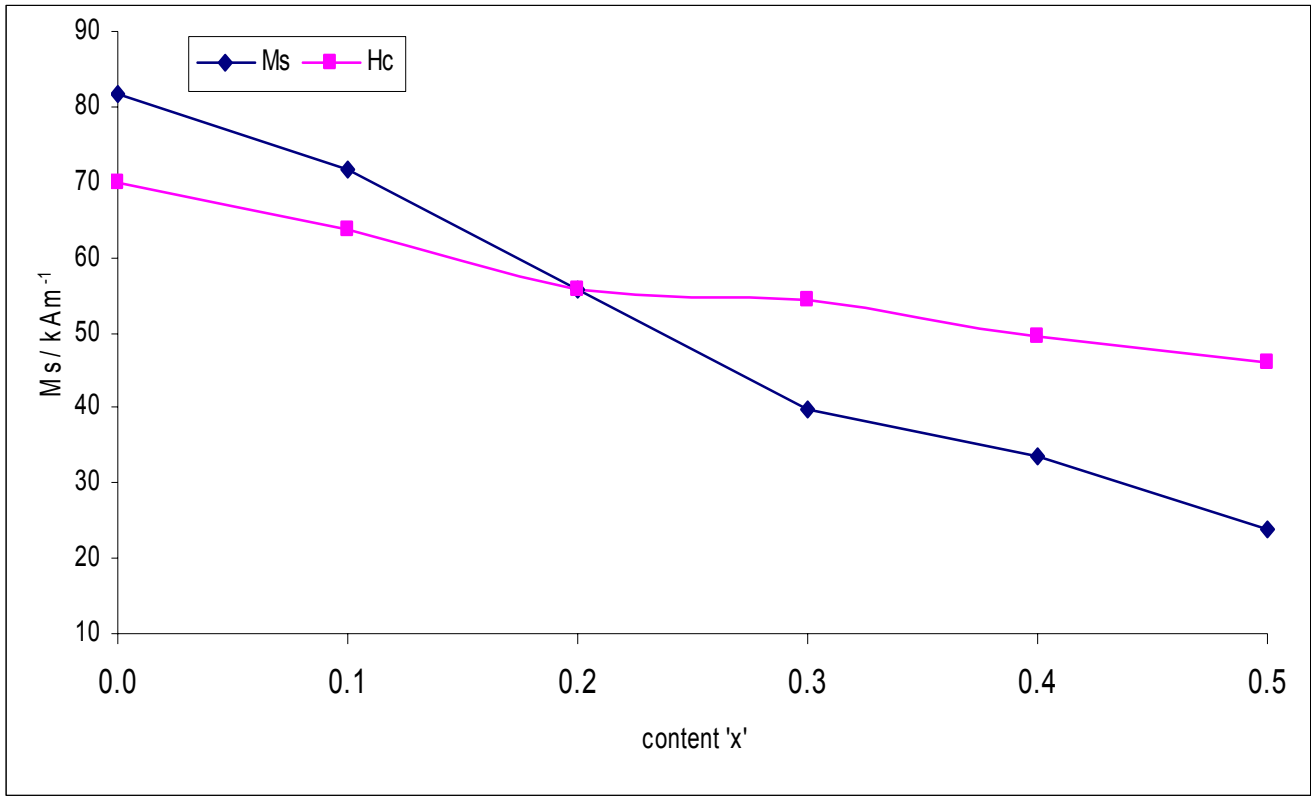

M_s= 81-23.89 kAm^{-1}(80.8 emu/g)

H_c= 70-46.18 kAm^{-1}

Calculated Y-K angles of Zr/Mg substituted cobalt ferrites

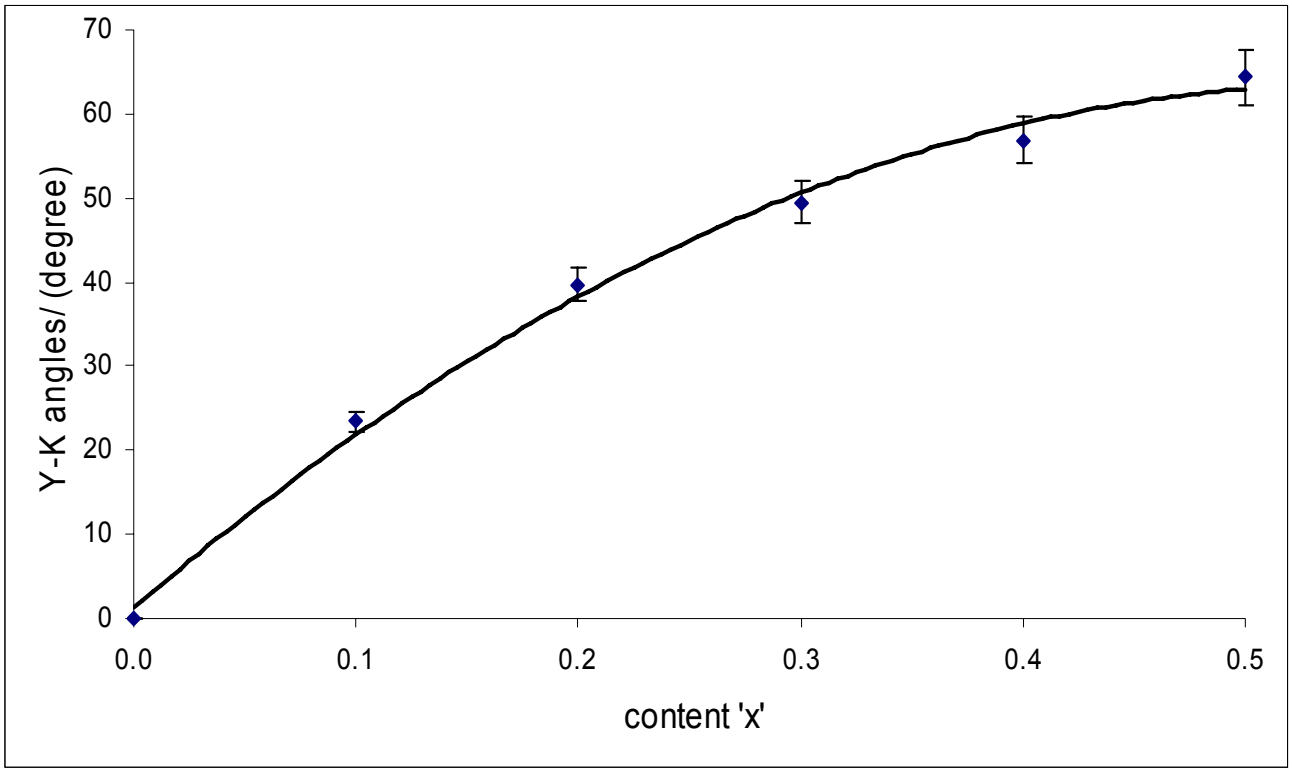

Conclusions for Zr-Mg doped cobalt ferrite

- All the samples synthesized are single spinel phase
- Resistivity increases (5.59×10^{7} to 2.75×10^{9} Ωcm) with increase in Zr-Mg content as expected
- Dielectric constant of the materials has shown irregular trend but overall show an increasing trend.
- The Curie temperature shows first increase (625K for x=0.1) and then decreasing trend with increase in Zr-Mg concentration (520K for x=0.5) (635 K for Cr doped sample)
- Zr-Mg addition was expected to increase the saturation magnetization but it has decreased the Ms value from 81 to 23.89 kAm^{-1}, suggesting that Neel's two sub-lattice model is not applicable. Yafet-Kittle model was applied to explain the decrease in Ms values.
- Yafet-Kittle angles varies from 23^{o}-64^{o}.

M.J. Iqbal; M.R. Siddiquah, *J. Magn. Magn. Mater.* 320 (2008) 845-850

Lithium Manganate Nanomaterials Doped with Rare-earth Elements

Properties of Lithium Manganate Spinel

- Most promising cathode materials for rechargeable Li-batteries
  - due to their elevated power density
  - low cost & environmental friendliness
- Small polaron semiconductor
- Low electrical resistivity ($10^5 \Omega cm$)
- High dielectric constant (~ 250)
- Low dielectric losses

Applications of Lithium Manganate Spinel

- Energy source for portable consumer devices (laptops, cameras, cellular phones, etc.)
- Automobile starters, hybrid electric vehicles (HEV),
- Uninterruptible power supplies (UPS)
- Discrete and multilayer chip (MLC) capacitor (cellular phones, military radio, etc.)
- Low loss substrate for microwave integrated circuits
- Microwave telecommunication applications (e.g. microwave antenna, receivers, etc.)
- Advanced microelectronics technologies such as dynamic random access memories (DRAM)

Objectives

- To synthesize stoichiometric, single-phase spinel nano-sized particles of lithium manganate and its doped derivatives
- To investigate the effect of rare-earth element (La, Ce, and Pr) as dopant on d.c. resistivity
- To enhance stability of spinel lattice in order to improve power capacity of batteries
- Investigation of dielectric properties

Work Plan

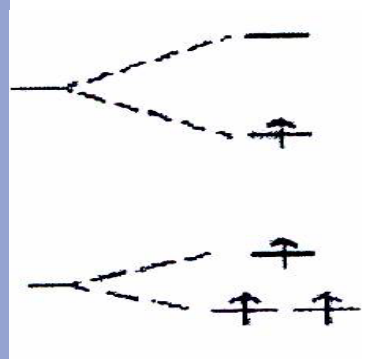

$LiMn_2O_4$

Mn^{3+} (High spin, $d^4, t_{2g}^3 e_g^1$)
Jahn-Teller active

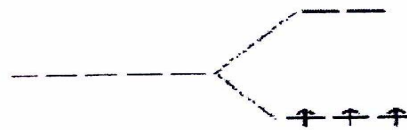

Mn^{4+}
(low spin, d^3, $t_{2g}^3 e_g^0$)
Jahn-Teller inactive

More important for odd number occupancy of the e_g level

More pronounced for complexes with 3 electrons in e_g level

$La^{3+=}(Xe)f$, $Ce^{3+}=(Xe)f^1$, $Pr^{3+}=(Xe)f^2$

- Jahn-Teller inactive
- Larger binding energy in MO_6 octahedral site

- Reduce the Jahn-Teller active Mn^{3+}ion
- Decrease the possibility of Jahn-Teller distortion but results in an increase in resistivity
- Increase the average ionic valance of Mn
- Stabilize the cubic structure

Experimental

Citrate sol-gel method

$LiNO_3$ (aq)+$Mn(CH_3COO)_2$ (aq) +$H_3C_6H_5O_7$

(1:2:3)

NH_3 | pH = 7

↓

Li(cit) + Mn(cit) + NH_4NO_3(aq)

120^{0}C | 8-10h

↓

$LiO.Mn_2O_3$ + H_2O

800 ^{o}C | 8 h

↓

$LiMn_2O_4$

Cit = $[C_6H_5O_7]^{3-}$

XRD patterns of $LiLa_xMn_{2-x}O_4$ samples where (a) x = 0.00, (b) x = 0.04, (c) x = 0.08, (d) x = 0.12, (e) x = 0.16 and (f) x = 0.20.

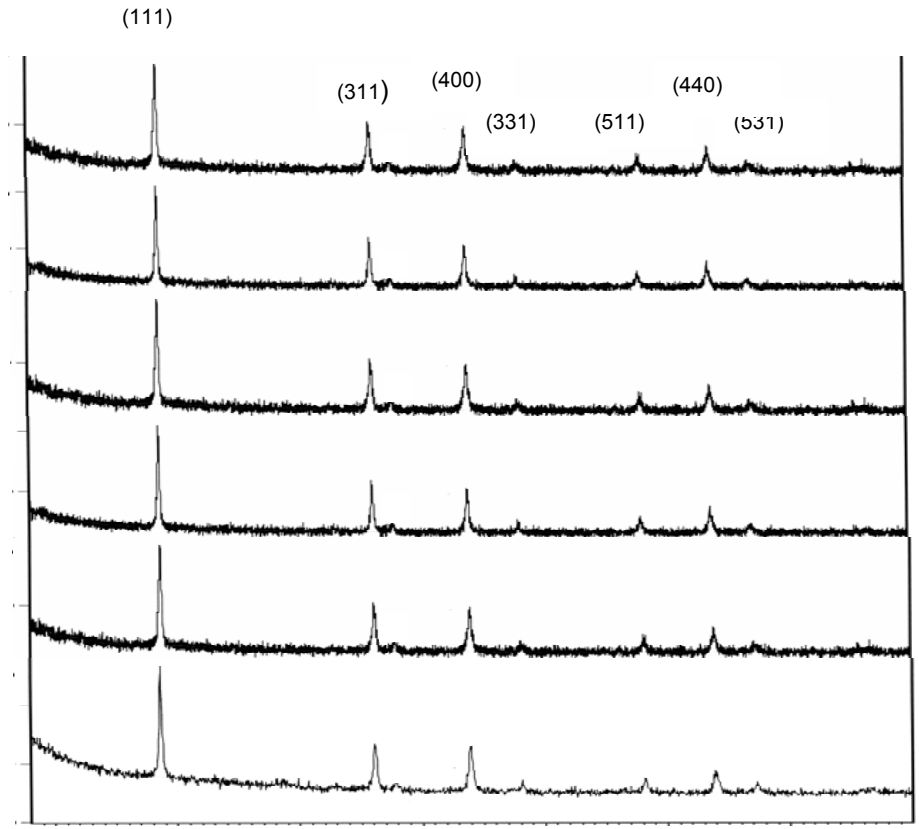

Parameters Calculated from XRD Data

Samples	Molar Mass (g/mol)	a/Å ± 0.01	V/Å^3 ± 0.01	D/nm ± 0.02	dx(g.cm^{-3}) ± 0.02
$LiMn_2O_4$	180.82	8.24	559.47	37	4.32
$LiLa_{0.04}Mn_{1.96}O_4$	184.18	8.22	555.41	27	4.41
$LiLa_{0.12}Mn_{1.88}O_4$	190.89	8.21	553.38	21	4.58
$LiLa_{0.20}Mn_{1.80}O_4$	197.61	8.19	549.35	27	4.75
$LiCe_{0.04}Mn_{1.96}O_4$	184.23	8.25	561.51	38	4.36
$LiCe_{0.12}Mn_{1.88}O_4$	191.04	8.23	557.44	25	4.54
$LiCe_{0.20}Mn_{1.80}O_4$	197.85	8.21	553.38	26	4.71
$LiPr_{0.04}Mn_{1.96}O_4$	184.27	8.24	559.47	26	4.40
$LiPr_{0.12}Mn_{1.88}O_4$	191.13	8.22	555.41	24	4.59
$LiPr_{0.20}Mn_{1.80}O_4$	198.01	8.20	551.36	25	4.77

Scanning electron micrographs of (a) $LiMn_2O_4$; (b) $LiLa_{0.04}Mn_{1.96}O_4$; (c) $LiCe_{0.04}Mn_{1.96}O_4$; (d) $LiPr_{0.04}Mn_{1.96}O_4$

- Homogenous phase
- Uniformly distributed particles
- Highly porous morphology

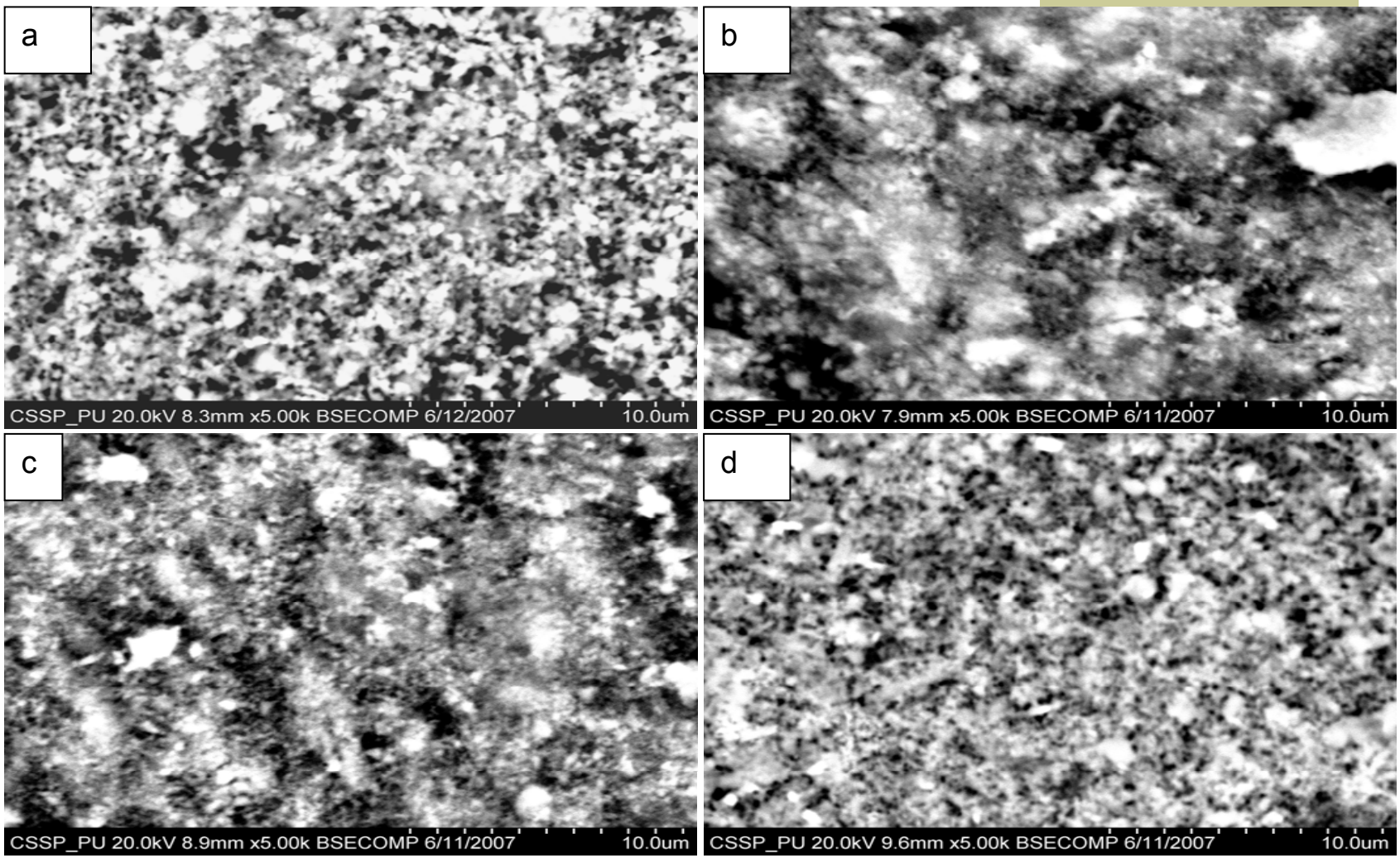

Plot of dc resistivity (a) and activation energy (b) Vs. dopant content, x

a

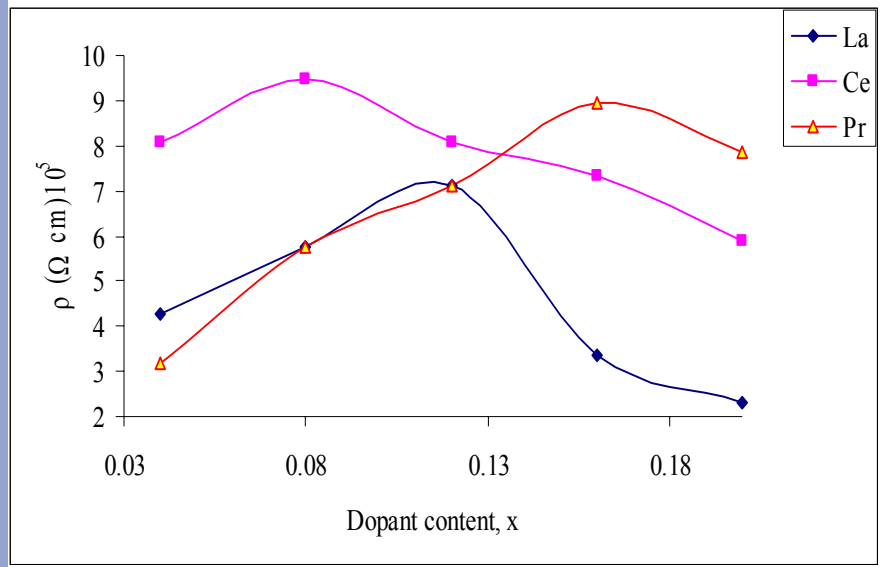

b

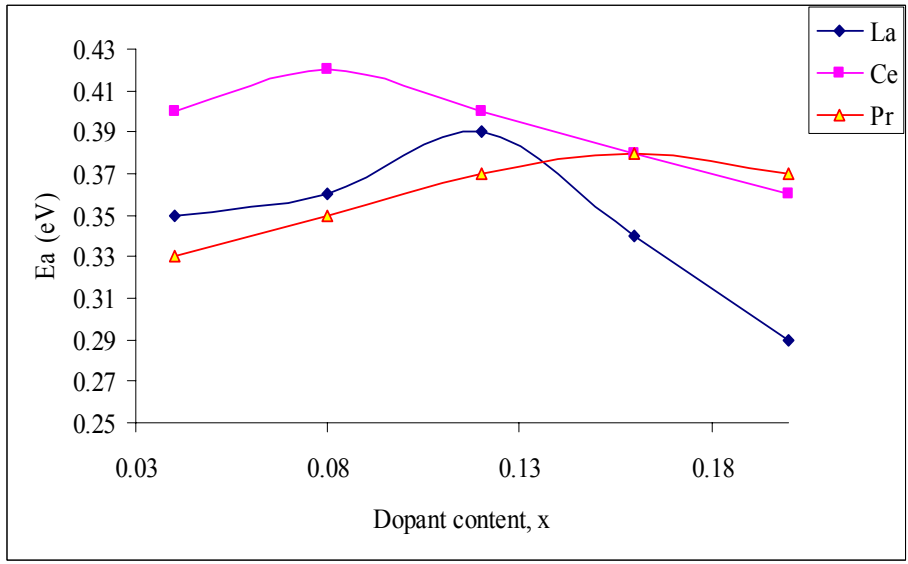

- ρ in the range of 10^5 Ωcm
- ρ increases up to x = 0.12
- ρ: Pr<La<Ce at x = 0.04

- Ea increases with dopant conc.
- Ea value ranges up to 0.3-0.4 eV

Initially the tetrahedral Mn^{3+}ions may have to shift to the octahedral site due to addition of dopant before the critical content and x >0.16 the dopants may not be able to occupy the octahedral site

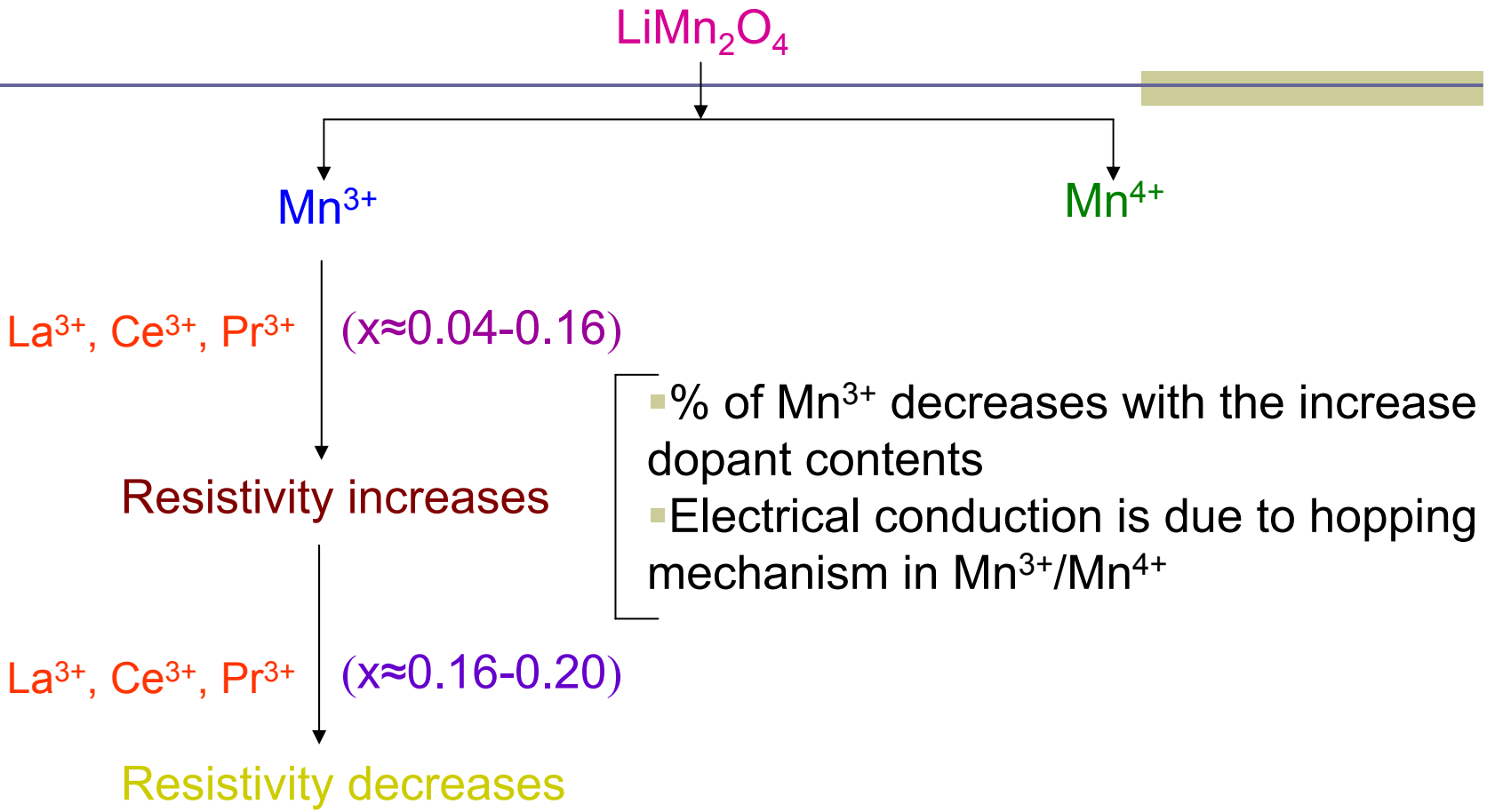

- % of Mn^{3+} decreases with the increase in dopant contents
- Electrical conduction is due to hopping mechanism in Mn^{3+}/Mn^{4+}

- The tetrahedral Mn^{3+}ions may have to shift to the octahedral site
- Dopant may not be able to occupy the octahedral site >0.16

Parameters Calculated from Dielectric Measurements

Dielectric parameters	f(MHz)	$LiMn_2O_4$	$LiLa_{0.04}Mn_{1.96}O_4$	$LiCe_{0.04}Mn_{1.96}O_4$	$LiPr_{0.04}Mn_{1.96}O_4$
ε	0.001	3.8×10^6	7.0×10^6	9.7×10^3	21.8×10^6
	0.1	830.41	903.53	478.50	1191.17
	1	124	127	62	**240**
tanδ	0.001	138	150	9.04	256
	0.1	2.27	3.19	0.94	4.26
	1	0.89	1.14	**0.64**	1.56

Conclusions

- All the samples are stoichiometric, single-phase spinel compounds with the crystallite size ranges 21-36nm
- Resistivity increases from (5.0×10^5 to 8.5×10^5 Ω cm) for x≤ 0.12
- The activation energy of hopping increases (0.39-0.42 eV) for x≤ 0.12
- Dielectric constant of the materials decreases with increasing applied frequency
- Pr-substituted spinel material is found to have maximum value of dielectric constant of 240, with dielectric loss of 1.56

M.J. Iqbal, Z Ahmad., ***J. Power Sources***, 179 (2008) 763-769

Spinel Magnesium Aluminate Nanomaterials

(By Sol Gel Method)

Magnesium Aluminate; $MgAl_2O_4$

Applications

- Refractory material and is used in cement rotary kilns, vacuum induction furnaces and glass industries
- Catalyst support in the field of environmental catalysis, petroleum processing and fine chemical production
- Humidity and gas sensing material


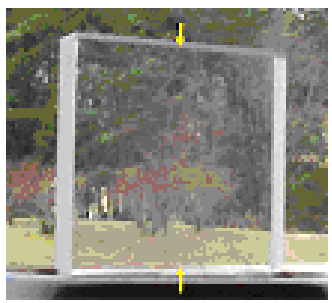

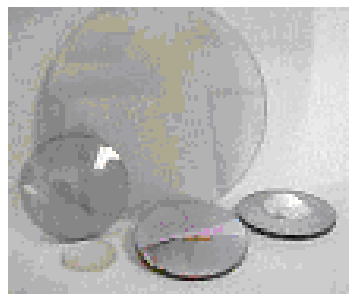

XRD patterns of $MgFe_xAl_{2-x}O_4$ samples where (a) x = 0.00, (b) x = 0.1, (c) x = 0.2, (d) x = 0.3, (e) x = 0.4, (f) x = 0.5, (g) x=0.6

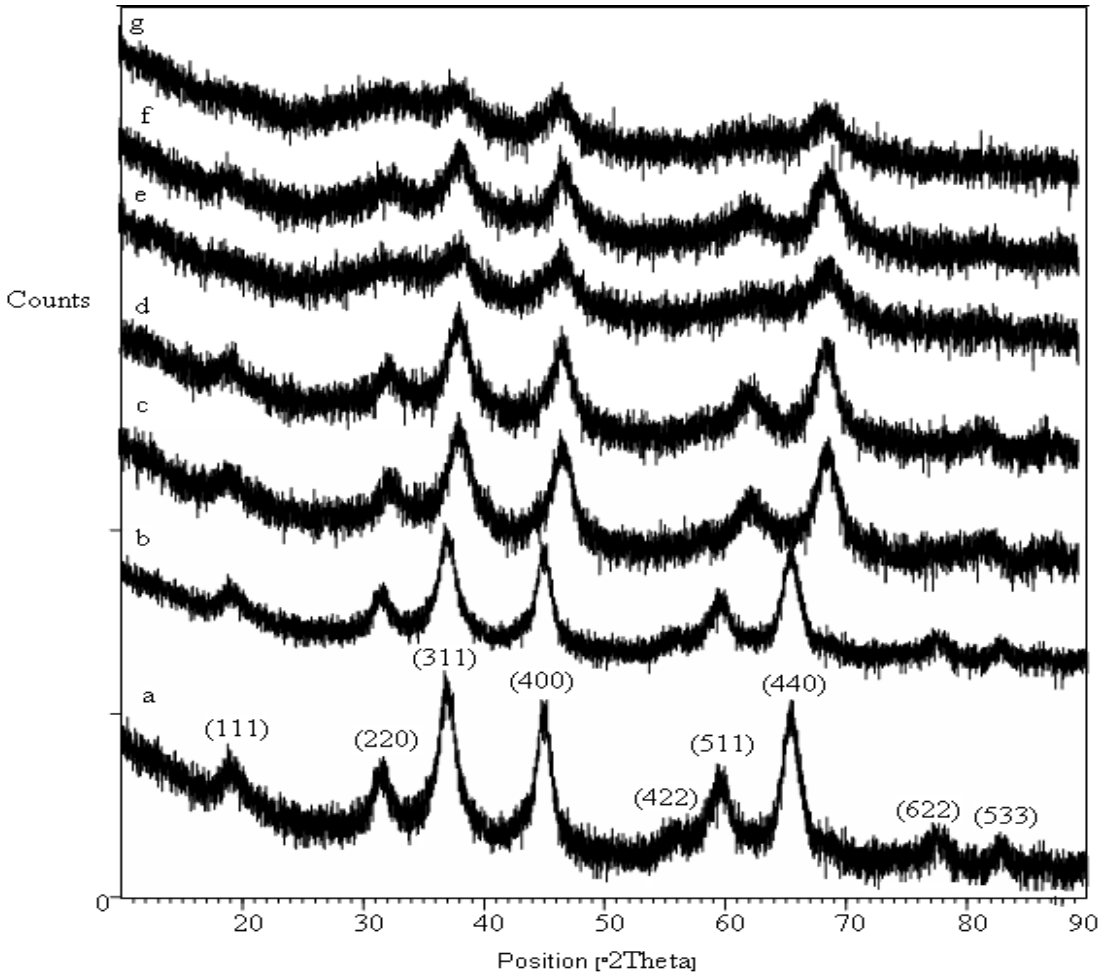

Scanning electron micrographs of $MgAl_2O_4$

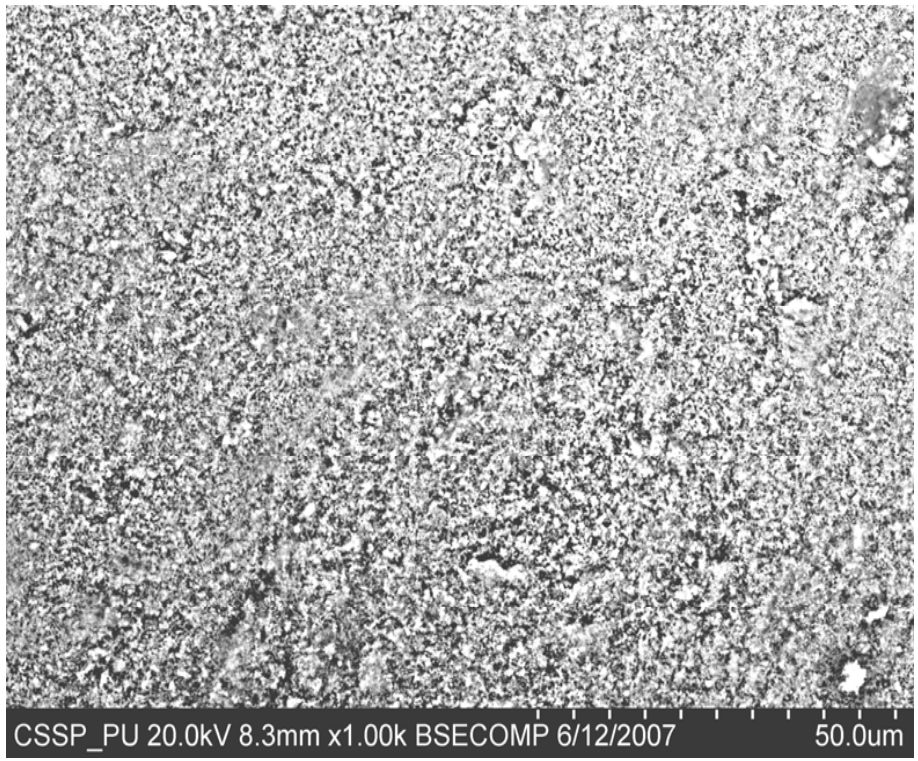

Parameters Calculated from XRD Data

Sample codes	Molar mass Values	a (Å)±0.043	V (Å³)	D (nm)	d_x (gcm^{-3}) ±0.064
$MgAl_2O_4$	142.0	8.056	522.8	12-18	3.621
$MgAl_{1.9}Mn_{0.1}O_4$	144.8	8.087	528.7	17-21	3.639
$MgAl_{1.9}Fe_{0.1}O_4$	144.9	8.083	528.5	15-19	3.643

Fig. (a, b) Plots of dc electrical resistivity for $MgAl_2O_4$ samples vs Temperature

a

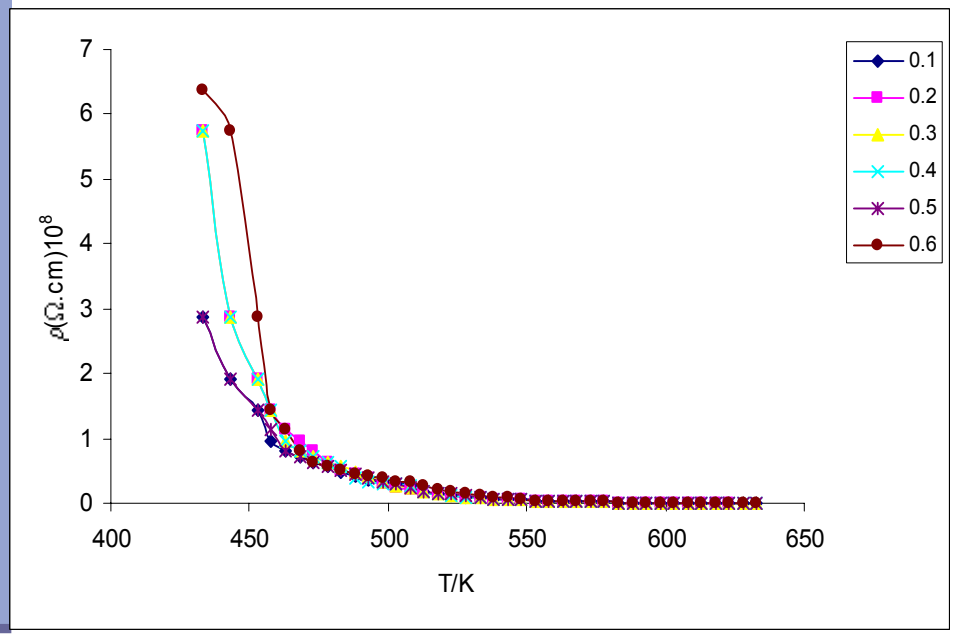

b

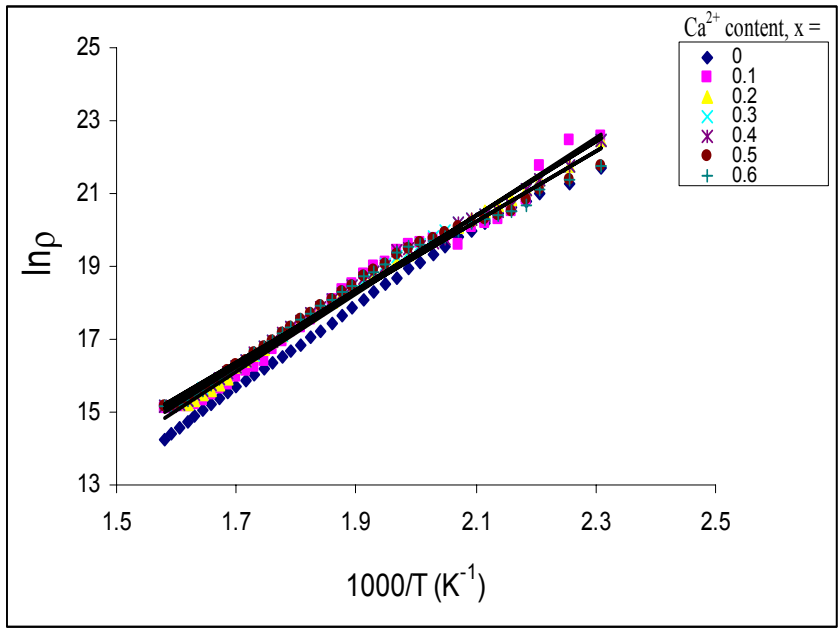

- ρ decreases on increasing temp.
- Semi-conducting behavior
- ρ ranges up to 10^8 ohm.cm
- Activation energy is directly related to dc resistivity

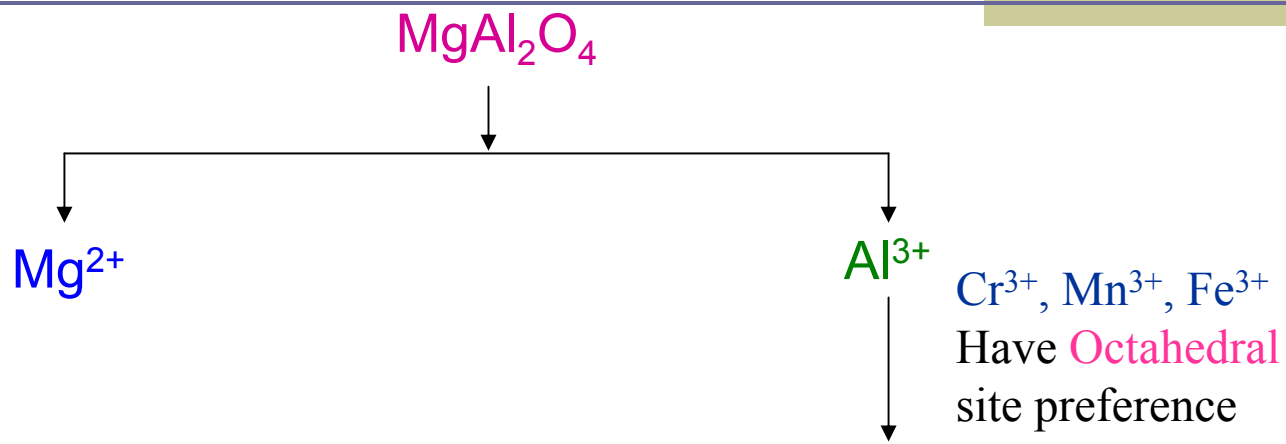

Resistivity decreases

- Electrical conduction is increased due to replacement of Al ions with Mn^{3+} and Fe^{3+} at the octahedral site

Parameters calculated by Resistivity Measurements

Samples	E_a /eV	Resistivity at 150°C ($\times 10^8 \Omega$cm) ±1.924
$MgAl_2O_4$	0.924	6.989
$MgAl_{1.9}Mn_{0.1}O_4$	0.692	1.414
$MgAl_{1.9}Fe_{0.1}O_4$	0.682	1.919

Conclusions

- All the synthesized samples are single-phase spinels with cubic symmetry
- Crystallite size ranges from 12-31 nm
- Particle size ranges from 40-55 nm by SEM
- X-ray density increases 3.505 to 3.692 gcm^{-3}
- Resistivity decreases $6.9\text{-}1.9 \times 10^{8} \Omega cm$ with increase in dopant content

M.J. Iqbal; S. Farooq, S., *Mater. Sci. Engg. B*, 136 (2007) 140-147

Effect of solution pH on the properties of $MgAl_2O_4$ and its derivative

Objectives

- To study the effect of pH on the formation and properties of nano sized spinel magnesium aluminates
- To determine the minimum pH required for the formation of the spinel single phase
- To study the electrical properties of the magnesium aluminates synthesized at different pH values (5-10)

Coprecipitation Method

$$Mg(NO_3)_2.6H_2O + 2Al(NO_3)_3.9H_2O + NH_4OH \longrightarrow MgAl_2O_4$$

(1:2 M)

$$Mg(NO_3)_2.6H_2O + 2Al(NO_3)_3.\ 9H_2O$$

pH (5-10) NH_4OH ↓ 1 hr stirring, aged overnight

$$Mg(OH)_2Al_2(OH)_6\ H_2O + NH_4NO_3\ (aq)$$

↓ Drying at 120°C/ 12hrs

$$MgO.Al_2O_3 + H_2O$$

↓ Annealing 950°C/ 8hrs

$$MgAl_2O_4$$

↓

Powdered (pelletized)

X-Ray Diffraction Patterns of Magnesium aluminate at pH 5 - 10

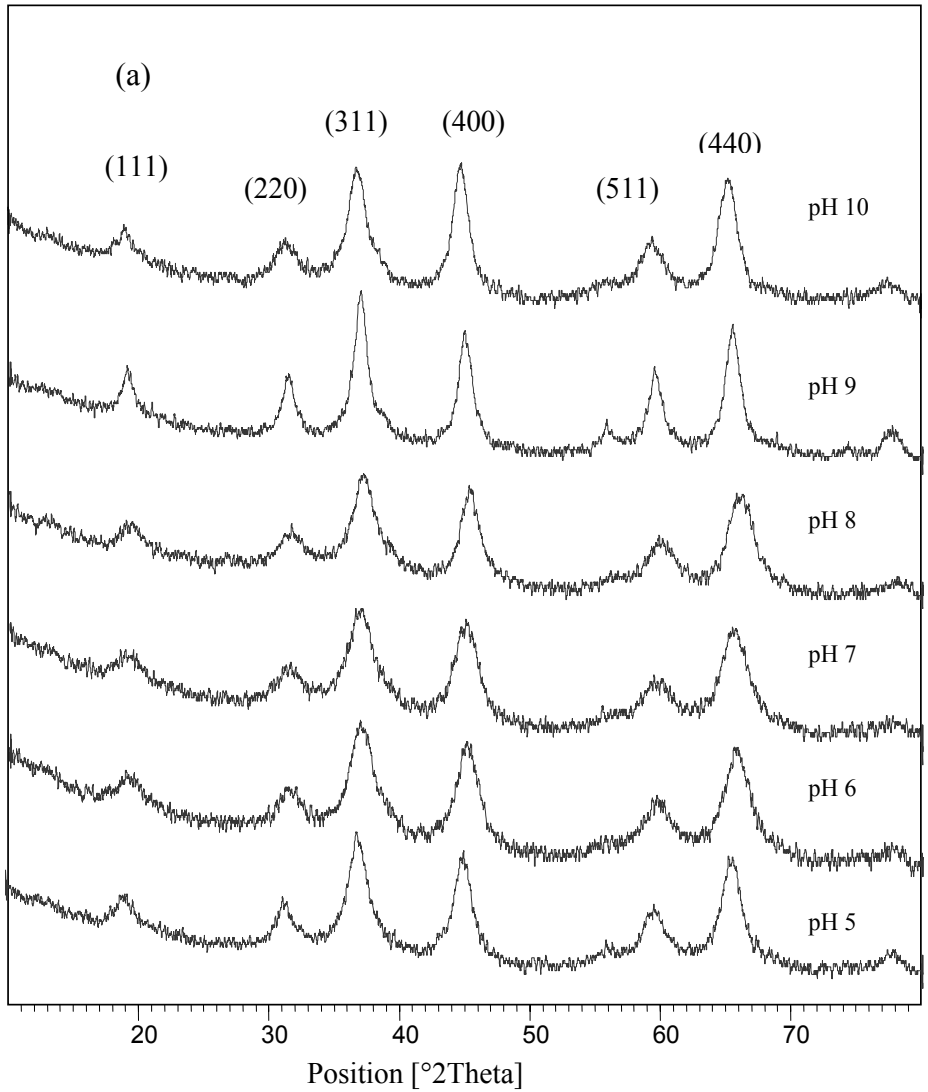

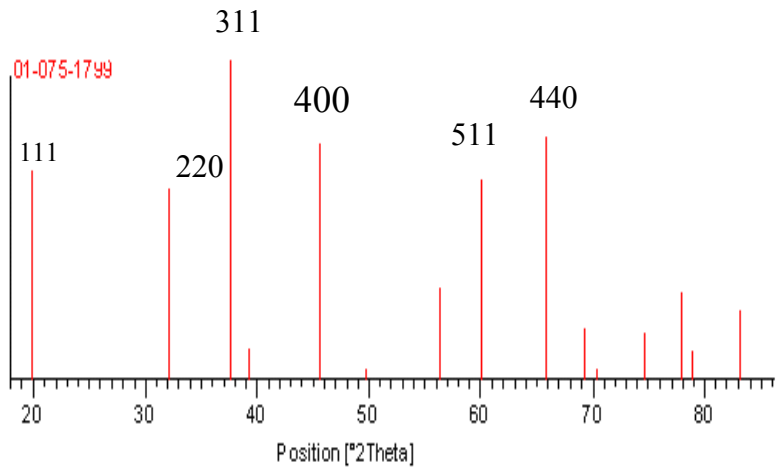

Thermal Analysis of Magnesium Aluminates at different pH

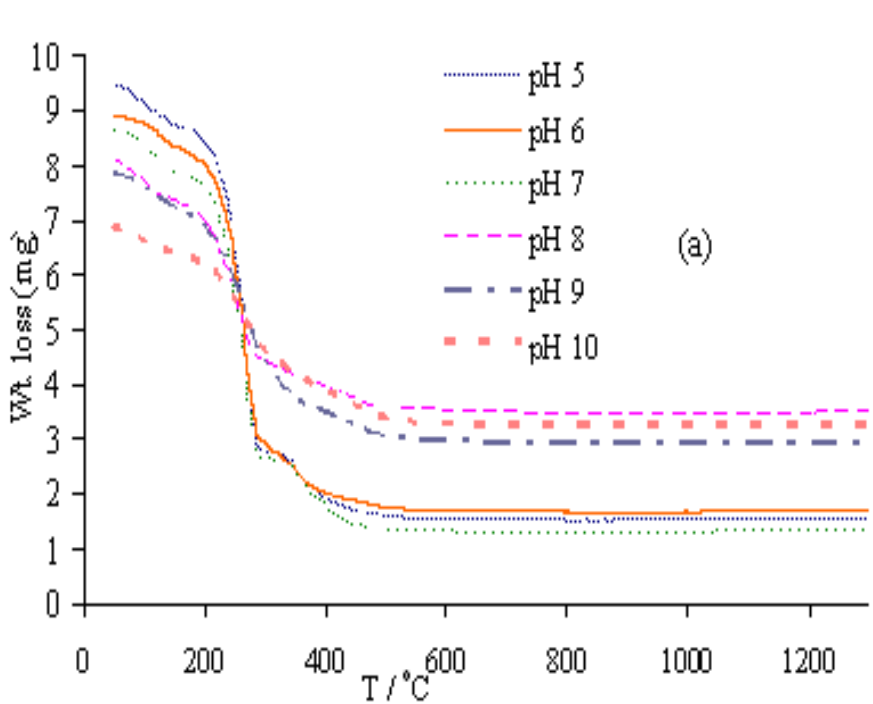

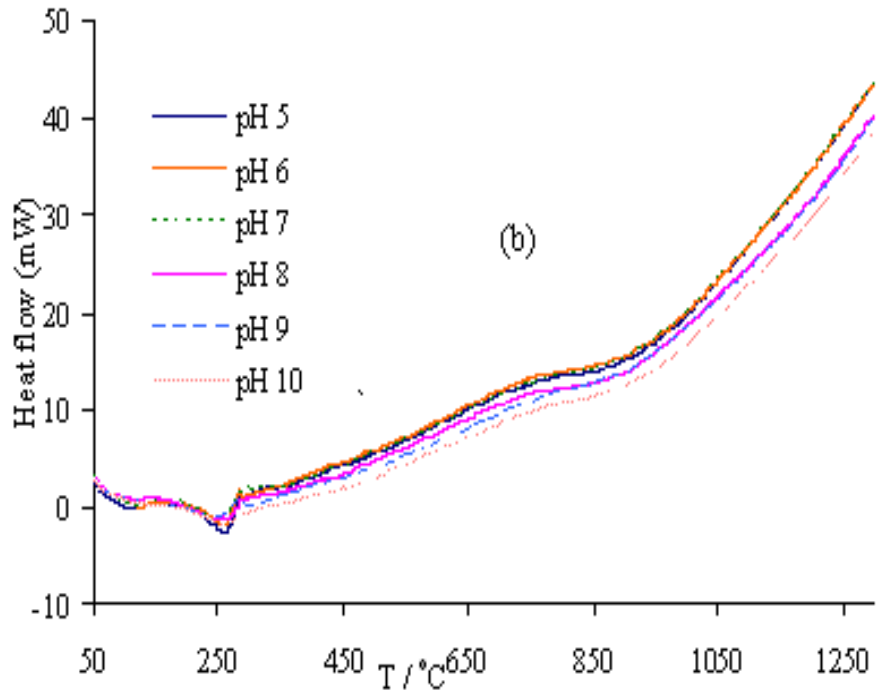

Electrical Properties

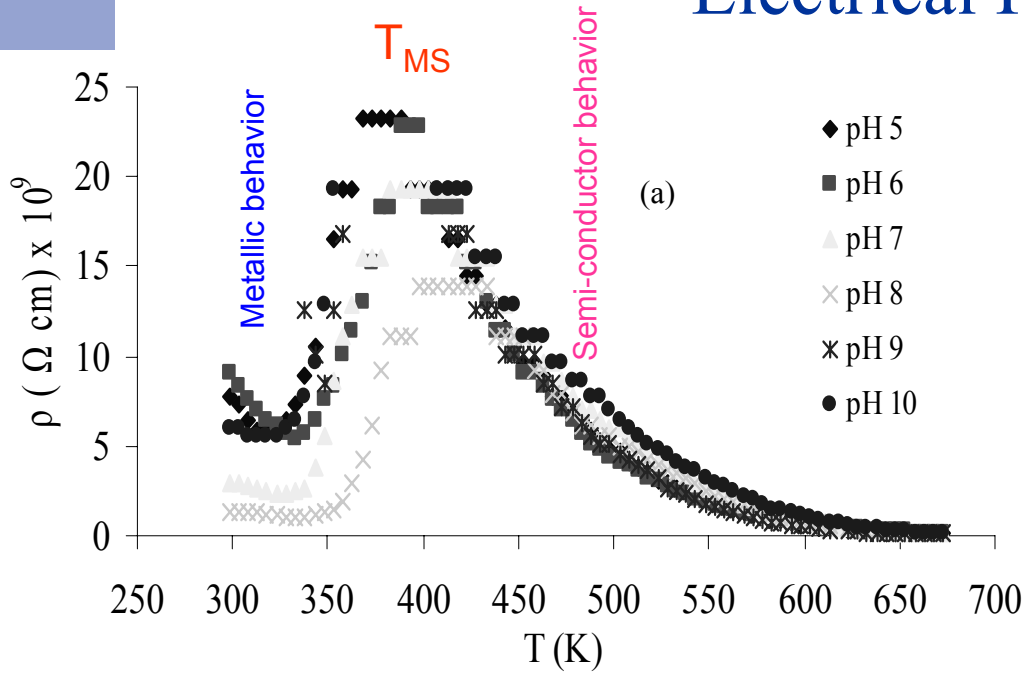

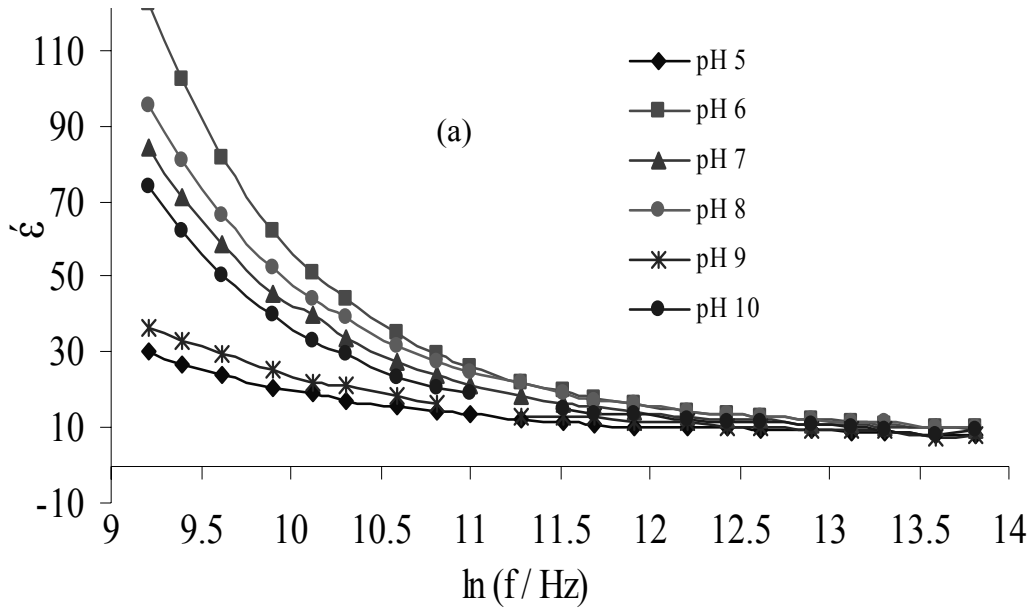

Resistivity and Dielectric constant values

pH	5	6	7	8	9	10
D (nm) (±2)	9-15	6-10	6-9	10-14	11-17	7-16
ρ (Ω cm)x10^9 (±1.26) at 350K	2.23	3.75	10.13	3.42	1.59*	2.9
έ (±0.15) 1MHz	8.26	9.88	9.51	10.21	8.09*	9.14

Conclusions

- Single phase spinel magnesium aluminate was successfully synthesized at the studied pH range of 5-10 by the coprecipitation method.
- Crystallite sizes obtained between 6 – 17 nm
- Resistivity values range between 1.59 – 10.13 x 10^9 Ohm.cm with the minimum value at pH 9.
- Dielectric constant values range between 8.26- 10.21 with a lowest value obtained at pH 9.

M.J. Iqbal; B. Ismail, *J. Alloy. Comp. (Submitted)*

THANKS

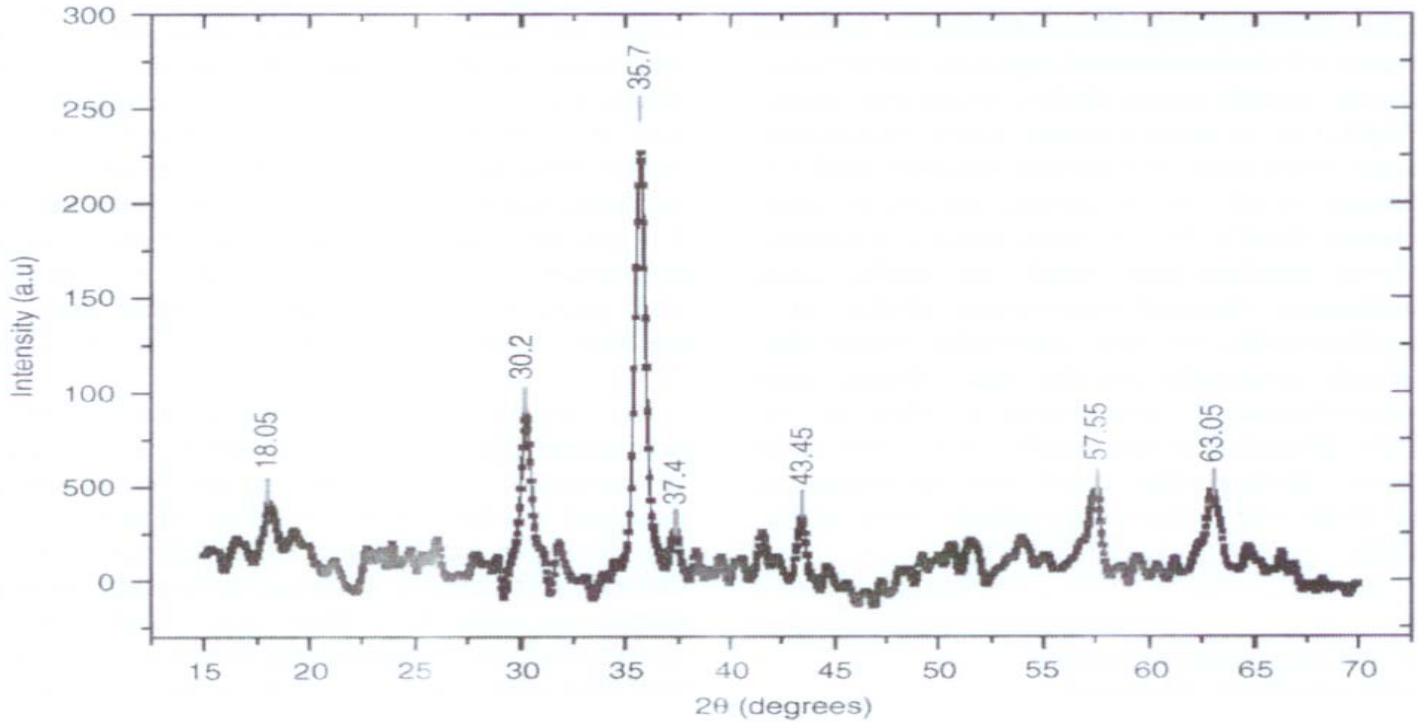

X-ray diffraction pattern of $CoFe_2O_4$ nanoparticles, average crystallite size, 21 nm.

K. Maaz et al. J. Magn. Magn. Mater. 308(2007)289-295

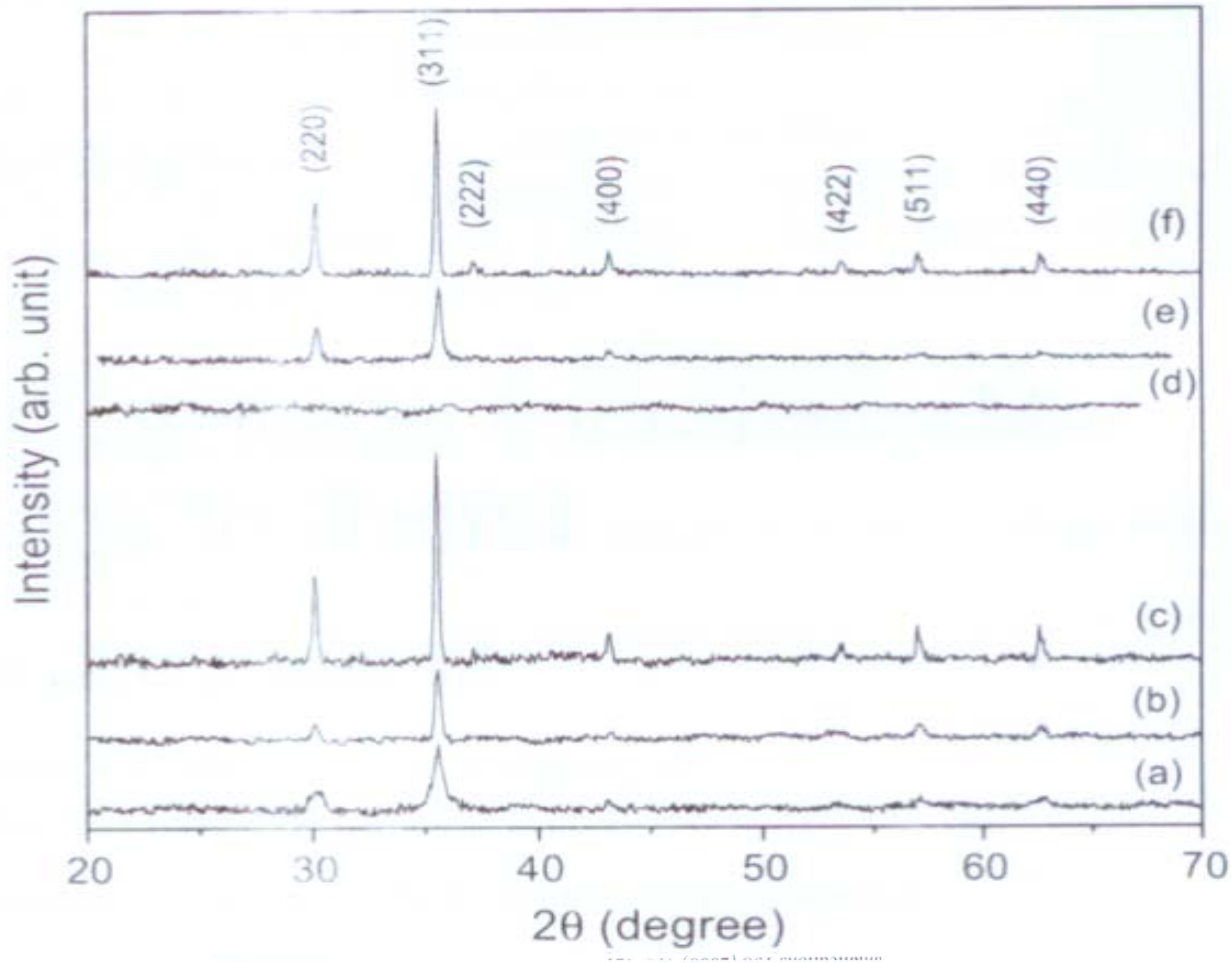

XRD patterns of $ZnFe_2O_4$ nanoparticles, average particle size, 18 – 52 nm

M. Atif et al. Solid State Comm. 138(2006)416-421.

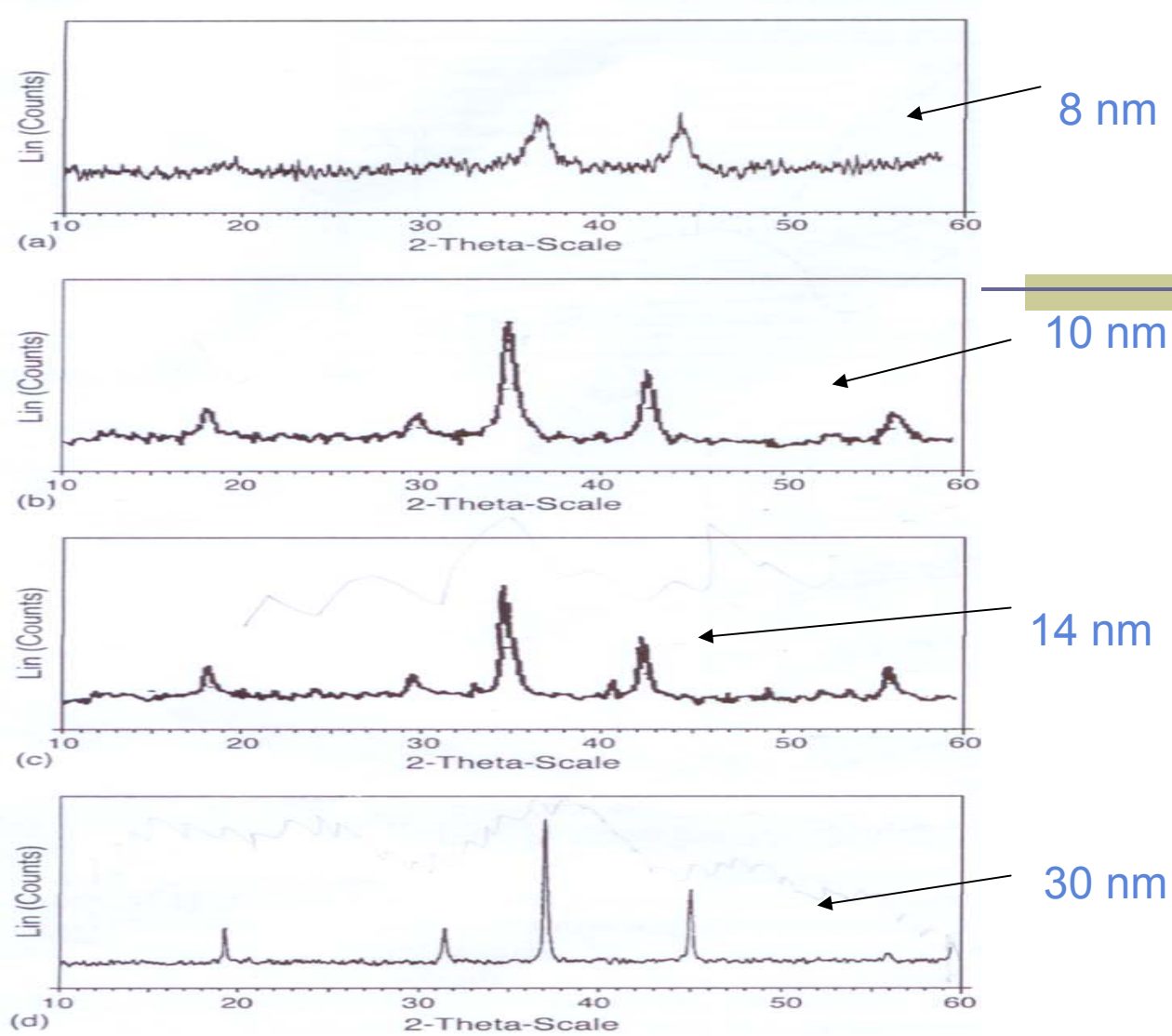

XRD patterns of $NiAl_2O_4$ nanoparticles, average particle size,
8 – 30 nm

S. Kurien et al. Mater. Chem. Phys. 98(2006)470-476.